

Article

Stripes Matter: Integrative Systematics of *Coryphellina rubrolineata* Species Complex (Gastropoda: Nudibranchia) from Vietnam

Irina Ekimova ^{1,*}, Yury Deart ² , Tatiana Antokhina ², Anna Mikhlina ³ and Dimitry Schepetov ¹

¹ Invertebrate Zoology Department, Lomonosov Moscow State University, Leninskie gori 1-12, 119234 Moscow, Russia; denlior@gmail.com

² A.N. Severtsov Institute of Ecology and Evolution, Leninskiy prosp. 33, 119071 Moscow, Russia; y.v.deart@gmail.com (Y.D.); tanya@sai.msu.ru (T.A.)

³ N.A. Pertsov White Sea Biological Station, Faculty of Biology, Lomonosov Moscow State University, Leninskie gori 1-12, 119234 Moscow, Russia; mikhleanna@gmail.com

* Correspondence: irenekimova@gmail.com

Abstract: *Coryphellina rubrolineata* (Gastropoda: Nudibranchia: Flabellinidae) was believed to be a widespread tropical species demonstrating high diversity in external and internal morphological traits. In this paper, we perform an integrative analysis of the *C. rubrolineata* species complex based on samples collected in Vietnam waters, combined with available data from other localities of the Indo-West Pacific. The methods of the study include morphological analysis of external and internal traits using light and scanning electron microscopy and the molecular analysis of four markers (COI, 16S, H3, and 28S). The phylogenetic hypothesis was performed using Bayesian and maximum likelihood approaches, and the species delimitation analyses included ASAP, GMYC, and bPTP. Our results support the validity of the genus *Coryphellina* as a distinct taxon and confirm that *Coryphellina rubrolineata* is restricted to the type locality and adjacent waters, while in the Indo-West Pacific, it represents a complex of pseudocryptic species. Based on our integrative analysis, we describe four new species: *Coryphellina pseudolotos* sp. nov., *Coryphellina pannae* sp. nov., *Coryphellina flamma* sp. nov., and *Coryphellina aurora* sp. nov. For the first time, *Coryphellina lotos* is reported in Vietnam waters. All five species differ in combination of coloration and other external traits and show minor differences in internal morphology.

Keywords: cryptic diversity; species delimitation; molecular phylogeny; chromatic variation; Indo-West Pacific; mollusca



check for updates

Citation: Ekimova, I.; Deart, Y.; Antokhina, T.; Mikhlina, A.; Schepetov, D. Stripes Matter: Integrative Systematics of *Coryphellina rubrolineata* Species Complex (Gastropoda: Nudibranchia) from Vietnam. *Diversity* **2022**, *14*, 294. <https://doi.org/10.3390/d14040294>

Academic Editors: Giulia Furfaro and Paolo Mariottini

Received: 19 March 2022

Accepted: 11 April 2022

Published: 13 April 2022

Publisher's Note: MDPI stays neutral with regard to jurisdictional claims in published maps and institutional affiliations.



Copyright: © 2022 by the authors. Licensee MDPI, Basel, Switzerland. This article is an open access article distributed under the terms and conditions of the Creative Commons Attribution (CC BY) license (<https://creativecommons.org/licenses/by/4.0/>).

1. Introduction

The advancement of DNA sequencing methods in taxonomical studies dramatically increased discovery rates of cryptic or pseudocryptic species complexes [1–3]. In morphology-based taxonomical studies, the presence of morphologically and ecologically diverse species has been widely accepted [4]. However, molecular systematics often demonstrates breaks in genetic diversity either across distant populations of putative widespread species [5–10] or within a single sympatric “population” demonstrating different ecological traits [11–14]. The existence of geographical barriers and allopatric speciation was believed to be the dominant driver for the diversification of widely distributed species; however, most recent studies highlighted the importance of ecological speciation for species living in sympatry and occupying different ecological niches [15,16]. In some cases, the cryptic or pseudocryptic diversity may be explained by a combination of different speciation scenarios [9].

The nudibranch *Coryphellina rubrolineata* O'Donoghue, 1929 (Gastropoda: Nudibranchia: Flabellinidae) was believed to have a very wide distributional range, being described from the Suez region in the Red Sea [17] and further reported from the Mediterranean

Sea (non-native population, see Gat [18], Yokes, Rudman [19]), the Red Sea [20,21], Indian Ocean [22–26], the Indo-West Pacific [27–31], subtropical waters of Korea [32], Japan [33], and Australia [34–36]. The main identification trait for this species was the presence of three red (commonly from pink to red-violet) lines continued along the dorsum and lateral sides of molluscs. However, in most regions, this species demonstrated several chromatic variations of body color (from white to purple) and cerata color (from translucent to orange, red, or violet) and different densities of dorsolateral red lines [37]. In 2017, a new species, *Coryphellina lotos* Korshunova et al., 2017, was described from the Pacific coast of Japan based on the integrative morphological and molecular analysis [38]. This species also possesses three red lines on dorsal and lateral sides, but those lines are discontinuous, suggesting that *Coryphellina rubrolineata* represents a species complex, and its chromatic variations in other regions require an additional study [38]. This view was confirmed in a subsequent work on the *Coryphellina rubrolineata* specimens collected from the type locality [39] (under the name *Flabellina rubrolineata*). It showed a clear separation of *C. rubrolineata* specimens collected in the Red Sea and the Arabian Sea from other specimens collected from the Indo-West Pacific and Australia. The authors highlighted that these results support the suggestion by Gosliner et al. [40] that “true” *C. rubrolineata* is restricted to the Red and Arabian seas and also non-natively occurs in the Mediterranean Sea, while in other regions it represents a complex of cryptic or pseudocryptic species [39].

The genus *Coryphellina* was recently re-established for flabellinids with papillate rhinophores and bilobed seminal receptaculum, following the integrative revision of the traditional family Flabellinidae [38]. This work showed polyphyly of traditionally defined genus *Flabellina* and suggested the major reclassification of this group with distinct families Apataidae, Samlidae, Unidentiidae, Flabellinopsidae, Paracoryphellidae, Coryphellidae, and Flabellinidae *s.str* and 27 genera. Although the validity of the families Apataidae, Samlidae, and Unidentiidae was widely accepted [40], the taxonomical changes within the rest of flabellinid diversity were taken with caution by some researchers [41–44]. Several subsequent works highlighted the suggested taxonomical scheme is excessively splitting and suggested synonymization of several flabellinid taxa (*Calmella* with *Flabellina*, Furfaro et al. [45]; all coryphellid genera with *Coryphella*, see Ekimova [46]; Ekimova et al. [44]). The identity of the genus *Coryphellina* also remains questionable, as few species have been studied to date, and it is not clear whether suggested synapomorphic traits are characteristic for all putative members of this genus.

Coryphellina rubrolineata was registered in Vietnam waters in 2012 (Martynov, Korshunova, 2012). However, consequent studies indicated that it was genetically distinct from the *C. rubrolineata* from the type locality, and differences in coloration suggested the presence of pseudocryptic species in this area [39]. Contemporary data on cladobranch diversity in Vietnam’s coastal waters remain incomplete and require de-dicated integrative studies [29,43]. From 2016 to 2021, 28 specimens of the genus *Coryphellina* were collected in different localities of Vietnam, 8 of them were identified as *Coryphellina exoptata* (Gosliner, Willan, 1991), and the rest belonged to the *Coryphellina rubrolineata* species complex. Some specimens of the latter species demonstrate similar external morphological traits (discontinuous dorsolateral lines) to *C. lotos* from Japan, and all specimens show high variation in coloration. The main goal of this study is to observe the potential cryptic diversity within the *Coryphellina rubrolineata* species complex in Vietnam based on integrative morphological and molecular analysis.

2. Material and Methods

2.1. Collection Data and Community Descriptions

A total of 28 specimens belonging to the genus *Coryphellina* were collected in 2016–2021 in various localities in the Southern (Phu Quoc, Tho Chu islands) and Central (Nha Trang Bay) Vietnam (Figure 1) during expeditions of the Vietnamese-Russian Tropical Centre. Most specimens were found in Nha Trang Bay, around Hon Tre, Hon Mot, and Hon Nok Islands. All specimens were collected during SCUBA diving at depths of 5–25 m. The

specimens were photographed and then fixed in either 96% ethanol or in 4% formaldehyde, in the latter case a piece of tissue was cut off and fixed in 96% ethanol for molecular analysis. Voucher specimens and DNA samples are stored in the collections of the Invertebrate Zoology department, Lomonosov Moscow State University (IZ). Type material is deposited in the collections of the Zoological Museum, Russian Academy of Science (ZIN). The collection of ZIN has policies to ensure compliance with laws governing the collection and sampling of wildlife from the country of origin and confirms that samples were legally imported to the museum repository where they are listed. Detailed sampling information and voucher numbers for each specimen are given in Table S1.

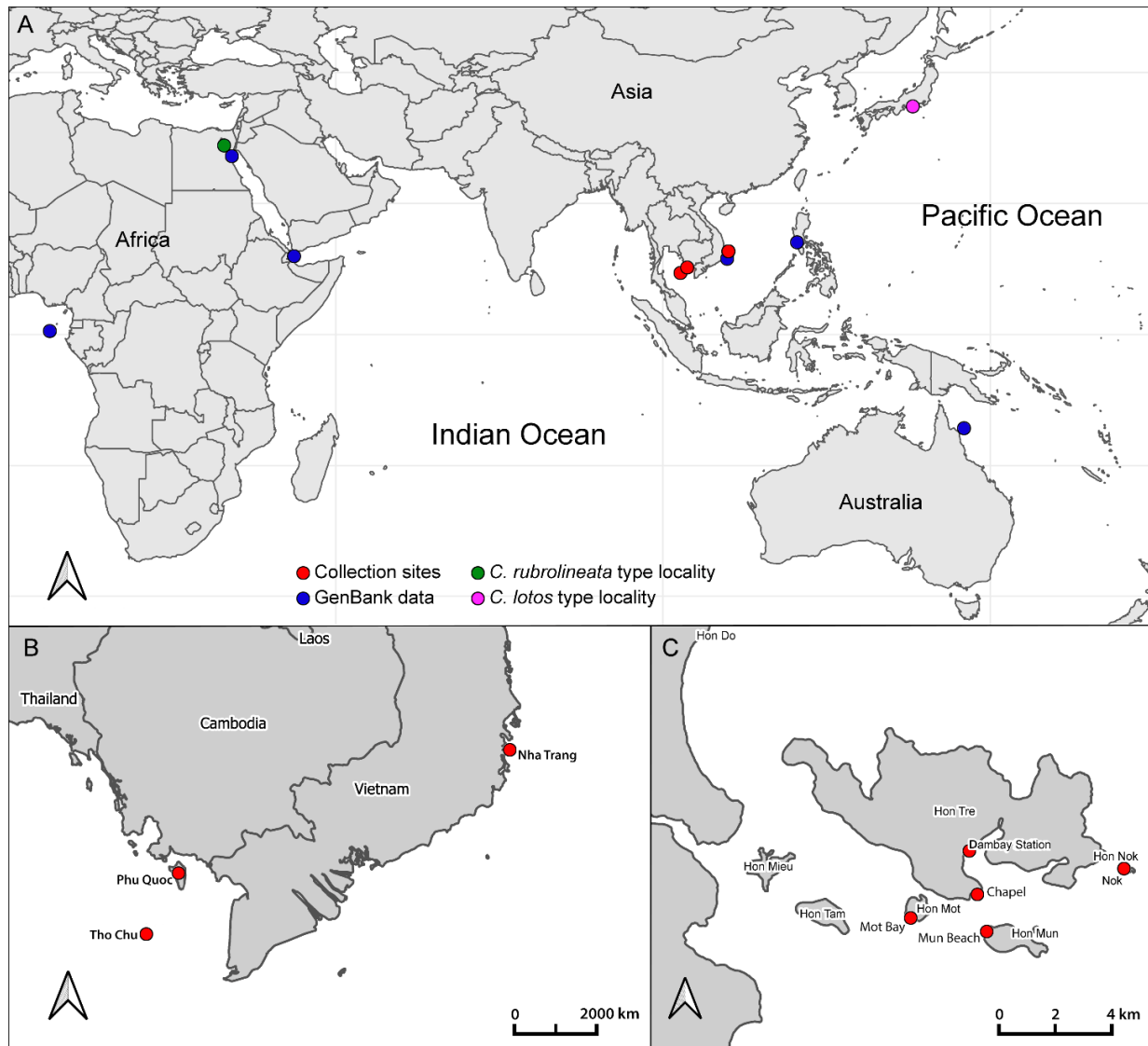


Figure 1. Collection sites of the studied material. (A)—Global map of the Pacific and Indian oceans with collection sites (red circles) and collection sites of samples from GenBank (blue circles). Green and magenta circles indicate the type localities of *Coryphellina rubrolineata* and *C. lotos*, respectively. (B)—Map of Southern and Central Vietnam. (C)—Map of collection sites in Nha Trang Bay.

2.2. DNA Extraction, Amplification, and Sequencing

Total genomic DNA was extracted from tissue samples preserved in 96% EtOH (Table S1) following the invertebrate protocol of the Canadian Center for DNA Barcoding [47]. Extracted DNA was used as a template for amplification of partial mitochondrial *cytochrome c oxidase* subunit I (COI) and 16S rRNA, and nuclear histone *H3* and 28S rRNA.

Reaction conditions and primers are shown in Table 1. Polymerase chain reactions were conducted with the “HS Taq” kit (Eurogen Lab, Moscow, Russia), following the manufacturer’s protocol. For sequencing, 1 to 2 μ L of amplicons were purified by ammonium acetate precipitation [48] and used for the sequencing reactions with the BigDye Terminator v3.1 sequencing kit by Applied Biosystems (Waltham, MA, USA). The reactions were analyzed using an ABI 3500 Genetic Analyser (Applied Biosystems) at N.K. Koltzov Institute of Developmental Biology RAS. All novel sequences were submitted to NCBI GenBank (Table S2).

Table 1. Amplification and sequencing primers and PCR conditions.

Marker	Primers	PCR Conditions	Reference
Cytochrome c oxidase subunit I	LCO1490 GGT CAA CAA ATC ATA AAG ATA TTG G HCO2198 TAA ACT TCA GGG TGA CCA AAA AAT CA	5 min—94 °C, 35 × [15 s—95 °C, 45 s—45 °C, 1 min—72 °C], 7 min—72 °C	[49]
16S rRNA	16Sar-L CGC CTG TTT ATC AAA AAC AT 16S R CCG RTY TGA ACT CAG CTC ACG	5 min—94 °C, 35 × [20 s—95 °C, 30 s—52 °C, 45 s—72 °C], 7 min—72 °C	[50,51]
Histone H3	H3AF ATG GCT CGT ACC AAG CAG ACV GC H3AR ATA TCC TTR GGC ATR ATR GTG AC	5 min—94 °C, 35 × [15 s—94 °C, 30 s—50 °C, 45 s—72 °C], 7 min—72 °C	[52]
28S rRNA	28SC1 ACC CGC TGA ATT TAA GCA T 28SC2 TGA ACT CTC TCT TCA AAG TTC TTT TC	5 min—94 °C, 35 × [15 s—94 °C, 30 s—50 °C, 45 s—72 °C], 7 min—72 °C	[53]

2.3. Data Processing and Phylogenetic Reconstruction

All raw reads for each gene were assembled and checked for ambiguities and low-quality data in Geneious R10 [54]. All edited sequences were checked for contamination using the BLAST-n algorithm run over the GenBank nr/nt database [55]. For phylogenetic reconstruction, molecular data from previous studies were added to the analyses [38,39]. All available sequences were aligned with the MUSCLE [56] algorithm in MEGA 7 [57]. For verification of reading frames and the presence of stop-codons, the COI and H3 sequences were translated into amino acids. Saturation was checked by plotting for all spe-cimens, including the outgroup of the total number of pairwise differences (transitions and transversions), against uncorrected p -distances. In the case of protein-coding markers, saturation was further examined separately for the first, second, and third codon positions. Sequences were concatenated by a simple biopython script following [58]. Phylogenetic reconstructions were conducted for the concatenated multi-gene partitioned data sets. The best-fit nucleotide evolution model for MrBayes phylogeny reconstruction method was selected in ModelTest-NG v0.1.7 [59,60] as follows: HKY+G+I for mitochondrial markers, K2+G+I for nuclear markers. Multi-gene analyses were performed by applying evolutionary models separately to partitions representing single markers. The Bayesian phylogenetic analyses and estimation of posterior probabilities were performed in MrBayes 3.2 [61]. The analysis was initiated with a random starting tree and ran for 10^7 generations. Maximum likelihood phylogeny inference was performed in the HPC-PHREADS-AVX option of RaxML HPC-PHREADS 8.2.12 [62] with 1000 pseudoreplicates under the GTRCAT model of nucleotide evolution. Bootstrap values were placed on the best tree found with SumTrees 3.3.1 from DendroPy Phylogenetic Computing Library 3.12.0. Final phylogenetic tree images were rendered in FigTree 1.4.0 and further modified in Adobe Illustrator CS 2015.

2.4. Species Delimitation

The COI alignment was used for computational species delimitations methods. *P*-distances were calculated using MEGA7 software [57]. To confirm the status of the clades recovered in our analysis as putative species, we used the Assemble Species by Automatic Partitioning (ASAP) method [63] to detect breaks in the distribution of intra- and interspecific distances without any prior species hypothesis, referred to as the “barcode gap” [64]. The ASAP analysis was run on the online version of the program (<https://bioinfo.mnhn.fr/abi/public/asap/asapweb.html>) (accessed on 1 March 2022) with the Jukes-Cantor (JC69) model. It was complemented by Poisson tree processes (PTP) [65]. The test was run using the bPTP Server <http://species.h-its.org/ptp/> (accessed on 1 March 2022) with 500,000 generations and with other settings set as default and with a COI-based maximum likelihood tree as an input. Additionally, we performed a GMYC test [66] and implemented it by the work of [67]. The COI-based ultrametric tree was calculated using BEAST 2.6.4 [68] with 107 generations and then analyzed in the R environment (package splits), following instructions by the work of [67]. Uncorrected *p*-distances in COI, H3, and 28S alignments were calculated in MEGA 7 [57].

2.5. Morphological Studies

All collected specimens were examined under a stereomicroscope. The internal morphology of 13 specimens was also studied, with closer attention to the digestive and reproductive systems. The buccal mass of each specimen was extracted and incubated overnight in proteinase K solution at 60 °C for dissolving the connective and muscle tissues, and then additionally soaked for 5 min in sodium hypochlorite. The radula and the jaws were rinsed in distilled water, air-dried, mounted on an aluminum stub, and sputter-coated with gold for visualization under a JEOL JSM 6380 scanning electron microscope (SEM, Jeol Ltd., Tokyo, Japan) and Tescan MIRA 3 LMH (Tescan, Brno, Czech Republic). General morphology of jaws and denticulation of masticatory border were examined by optical stereomicroscopy and SEM. For the study of the reproductive system, specimens were dissected from the dorsal side along the midline and examined under a stereomicroscope.

2.6. Nomenclatural Acts

The electronic edition of this article conforms to the requirements of the amended International Code of Zoological Nomenclature (ICZN), and hence the new names contained herein are available under that code from the electronic edition of this article. This published work and the nomenclatural acts it contains have been registered in ZooBank, the online registration system for the ICZN. The LSID for this publication is: urn:lsid:zoobank.org:pub:0A201DEA-A909-42EB-85F2-8294E7690170.

3. Results

3.1. Phylogenetic Analysis

Trees based on the single-gene analyses were poorly resolved (Data S1); however, the concatenated tree provided suitable resolution for most clades (Figure 2). The topology of the concatenated trees generated with the Bayesian inference (BI) and the maximum likelihood (ML) analyses was congruent (Figure 2, Data S1). In our analysis, the genus *Coryphellina* was recovered as monophyletic, with high statistical support (PP (posterior probability from the Bayesian inference) = 1; BS (bootstrap support from maximum likelihood) = 100). On the tree, a total of eight distinct clades containing putative *Coryphellina* species were recovered, but only two of them strictly corresponded to the initial species hypothesis: *Coryphellina arveloi* (Ortea and Espinosa, 1998) (PP = 1; BS = 100) and *C. exoptata* (PP = 1; BS = 100). Specimens of *C. lotos* were grouped into two distinct and highly supported clades: one clade was represented by the type specimen (ZMMU Op-515) and five specimens from Vietnam (PP = 1; BS = 100). Smaller specimens from Vietnam were grouped with “*C. rubrolineata*” from GenBank collected in Queensland, Australia (PP = 1; BS = 96). *Coryphellina rubrolineata* was represented by four highly supported groups and

two singletons. Specimens collected close to the type locality (*Coryphellina rubrolineata* IEfr1, IEfr2) represented a separate clade (PP = 1; BS = 100), which was sister to a sample from Sulawesi (ZFMK262). Specimens from Vietnam formed two distinct clades (PP = 1; ML = 100 in both cases) and one singleton. The deep relationships within “*rubrolineata*” and “*lotos*” species complexes are mostly unresolved, but all species together form a highly supported clade (PP = 1; BS = 98). In summary, our analysis indicates the presence of eight putative species of *C. rubrolineata* species complex (including *C. lotos*), represented by highly supported clades or derived singletons. Same results were received in the analysis of trees based on single-gene data sets (Data S1).

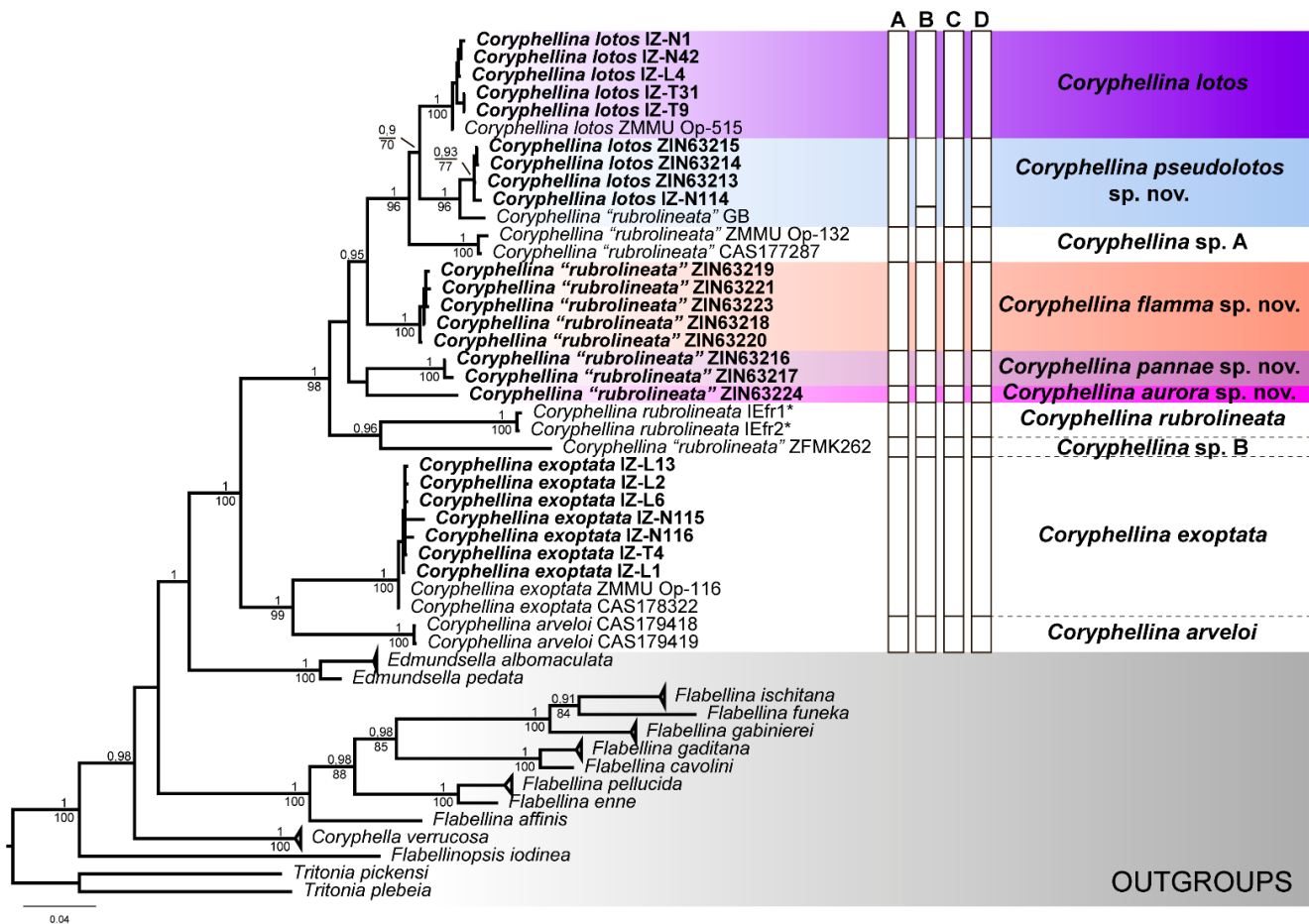


Figure 2. The Bayesian phylogenetic tree of the genus *Coryphellina* based on the concatenated data set of four markers (COI+16S+H3+28S). Specimens in bold are studied in this work. The taxa labels on the tree indicate the initial identification of the specimens, and species names on the right indicate the revised species hypothesis. White blocks correspond to results of species delimitation analyses: (A)—ASAP ($p = 1.06$, score 1.5); (B)—ASAP ($p = 2.12$, score 1.5); (C)—bPTP; (D)—GMYC. Numbers above branches indicate posterior probabilities of the Bayesian inference, numbers below—bootstrap support from the maximum likelihood. A star (*) indicates the nominative species *Coryphellina rubrolineata*, collected near the type locality.

3.2. Species Delimitation

The initial species hypothesis implied the presence of 10 monophyletic units recovered in the phylogenetic analysis: *Coryphellina rubrolineata* (from the type locality), *C. lotos* (clade comprising the type material), *C. exoptata*, *C. arveloi*, and 6 candidate species from *C. rubrolineata* species complex (Figure 2). The ASAP analysis (Figure S1) showed the lowest ASAP score (1.5) for the two hypotheses: one corresponded to the initial species hypothesis with 10 candidate species, and in the second hypothesis, the single specimen from GenBank (COI accession KJ001316) represented a separated species, implying 11 candidate

species. The same 11 candidate species were identified in the bPTP (Figure S2) and GMYC (Figure S3) analyses. This result was also supported by the calculated uncorrected *p*-distances in COI, H3, and 28S markers. The intraspecific variability of COI markers within candidate species did not exceed 4.2%, and the interspecific distances varied between 9.38% and 16.79% (Table S3). It should also be noted that in most cases, the H3 and 28S data set showed high genetic variation, as interspecific pairwise distances between putative species of *C. rubrolineata* species complex varied from 0% to 4.29% in the case of the H3 data set and from 0.37% to 13.28% in the case of 28S.

To sum up, we can conclude that the diversity of *Coryphellina rubrolineata* species complex in Southern Vietnam represents a complex of cryptic and pseudocryptic species, including *C. lotos* and four new distinct species, which are formally described below. We also identified two other new species, but since their material was not available for morphological study (only sequences from GenBank), their formal taxonomical description is a prospect for future studies.

3.3. Systematics

Order Nudibranchia Blainville, 1814

Suborder Cladobranchia William and Morton, 1984

Superfamily Fionoidea Gray, 1857

Family Flabellinidae Bergh, 1889

Genus *Coryphellina* O'Donoghue, 1929

Diagnosis (from Korshunova et al. [38] with modifications): Body narrow. Notal ridge present, reduced, discontinuous, in several indistinct pieces. Cerata on low elevations, in several groups. Rhinophores similar in length or shorter than oral tentacles, densely papillated. Anterior foot corners present. Anus pleuroproctic. Distinct oral glands. Rachidian teeth with narrow compressed cusp and distinct denticles. Lateral teeth denticulated with attenuated process basally. Proximal receptaculum seminis bilobed. Distal receptaculum seminis present. Short prostatic vas deferens. Penis conical to bulbous.

Type species: *Coryphellina rubrolineata* O'Donoghue, 1929

3.3.1. *Coryphellina lotos* Korshunova, Martynov, Bakken, Evertsen, Fletcher, Mudianta, Saito, Lundin, Šchrödl, and Picton, 2017

Material studied: **IZ-T31**, 1 specimen, dissected, 17 mm in length preserved, Vietnam, Nha Trang, Hon Tre, coordinates and depth unknown, 29 October 2015 coll. E.S. Mekhova. **IZ-N1**, 1 specimen, 12 mm in length preserved, Vietnam, Nha Trang, Hon Mot, N 12°10'27.56" E 109°16'19.61", 16 m in depth, on rocks, 30 March 2016, coll. Y.V. Deart. **IZ-N42**, 1 specimen, dissected, 17 mm in length preserved, Vietnam, Nha Trang, Dambay, N 12°11'39.84" E 109°17'26.74", 5–6 m in depth, on net in sand, 9 April 2016 coll. Y.V. Deart. **IZ-T9**, 1 specimen, dissected, 19 mm in length preserved, Vietnam, Nha Trang, Hon Mun, N 12°10'026" E 109°17'725", 10–18 m in depth, stone on silty bottom, 25 October 2016 coll. V.O. Barkalova. **IZ-L4**, 1 specimen, dissected, 23 mm in length preserved, Vietnam, Nha Trang, Hon Tre, N 12°10'54.95" E 109°17'37.94", 10 m in depth, 2 April 2019, coll. E.S. Mekhova.

External morphology (Figure 3): Length up to 23 mm (preserved). Body slender, foot slender with long anterior corners. Oral tentacles 1.5–2 times longer than rhinophores. Rhinophores highly papillated, bearing up to 70 papillae on inner side. Cerata cylindrical, pointed distally, elongated, arranged in distinct groups. Up to six groups of cerata per row. First group largest, with 9–13 cerata in group. Second group with 4–5 cerata. Cnidosacs on top of cerata. Digestive gland diverticula cylindrical, fill about 1/4–1/3 of ceratal volume. Well-defined discontinued notal edge under ceratal groups. Anus pleuroproctic. Reproductive openings lateral, below first group of cerata.

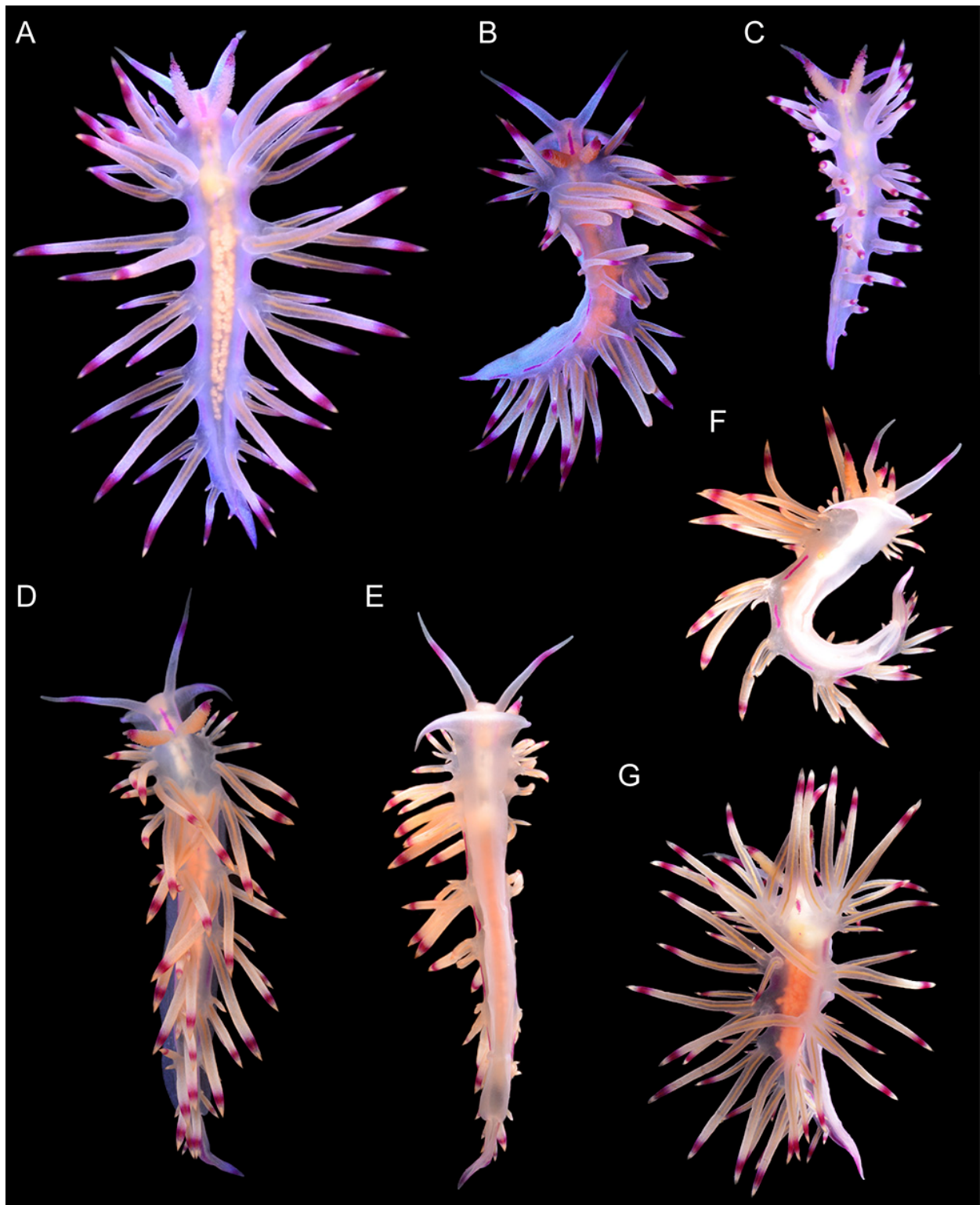


Figure 3. *Coryphellina lotos*, external morphology and variability of coloration. (A)—IZ-T9, specimen 19 mm in length (preserved). (B)—IZ-T31, specimen 17 mm in length (preserved). (C)—IZ-N1, specimen 12 mm in length (preserved). (D)—IZ-N42, specimen 17 mm in length (preserved), dorsal view. (E)—IZ-N42, ventral view. (F)—IZ-N42, lateral view. (G)—IZ-L4, specimen 23 mm in length (preserved). Photo credits: (A,G): Elena Mekhova; (B): Tatiana Antokhina; (C–F): Yury Deart.

Color (Figures 3 and 4): Background from translucent white to violet and purple. Digestive gland mass and diverticula in cerata from peachy to light brown. Cerata peachy

to purple, cnidosac area covered by peachy pigment with intense red to violet subapical rings. Underneath subapical rings, cerata covered by sparse white opalescent speckling. Prominent thick pink line beginning between oral tentacles, line on body indistinct, discontinuous. Pink to lilac discontinuous lines located laterally in ceratal intergroup space under notal edge, continuing from head to tail. Tip of tail same color as lines. Rhinophores same color as body or apricot, with translucent tips and pink to purple subapical rings. Oral tentacles white to purple, covered by sparse white opalescent powder in middle, with intensive pink to purple subapical rings and translucent tip.

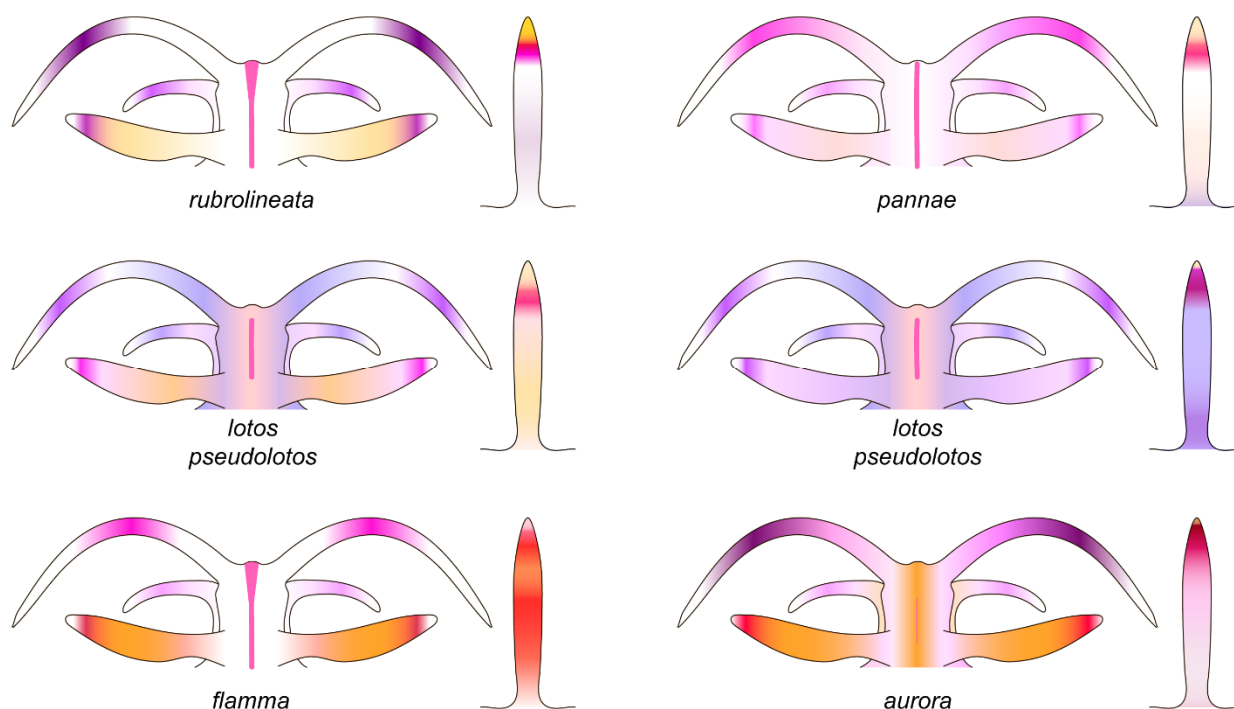


Figure 4. Diagrams of the color pattern of head region and cerata in *Coryphellina rubrolineata* species complex.

Internal morphology (Figures 5, 6B and 7A): Jaws composed of two triangular plates with triangular masticatory process (Figure 5A). Masticatory process with numerous sharp denticles, arranged in up to five rows, outermost denticles largest with secondary denticles, innermost blunt (Figure 5B). Radula triseriate, radular formula: $27\text{--}35 \times 1.1.1$ (Figure 5C–H). Rachidian tooth elongated-triangular with short conical central cusp, bearing 5–7 large denticles with deep furrows on both sides. Cusp sharp, small, slightly compressed by adjacent denticles. Lateral teeth of widened triangular shape with elongated cusp and 7–11 denticles on inner edge. Base of teeth almost right angled proximally, oblong distally, with long attenuated processes. Small denticles on outer tooth side (Figure 5E). Reproductive system diaulic (Figure 7A). Ampulla large, sausage-shaped, widened in middle. Proximal seminal receptacle bilobed. Vas deferens slightly widens distally before entering penial sac, presenting prostatic area. Mucous gland lays distally into vagina, albumen, and membrane glands next to proximal seminal receptacle. Their connection to vagina is not clear. Distal seminal receptacle small, opened into vagina distally. Penis small, conical, unarmed.

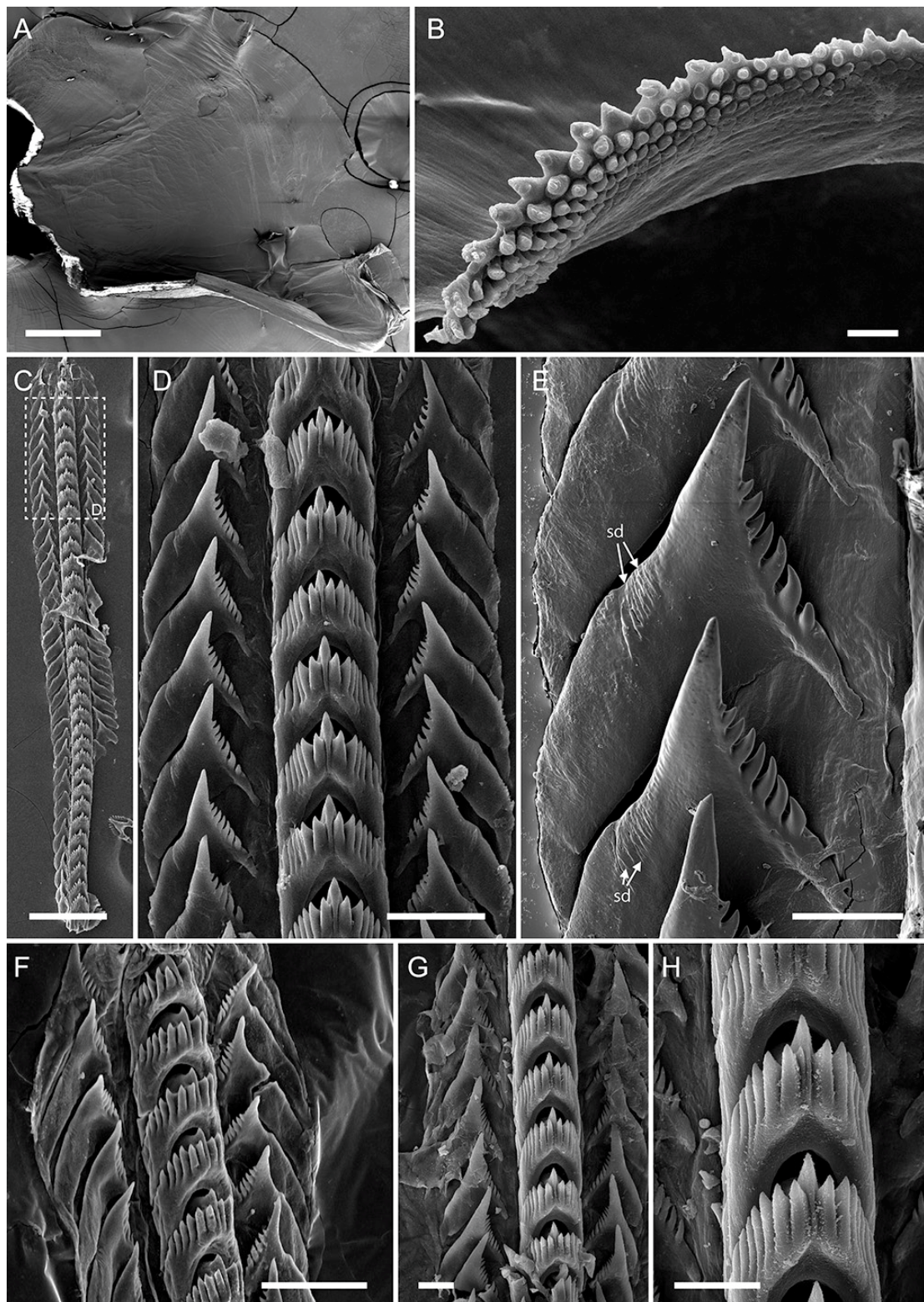


Figure 5. *Coryphellina lotos*, buccal armature. (A)—IZ-L4, specimen 23 mm in length (preserved), right jaw plate. (B)—IZ-L4, masticatory process denticulation. (C)—IZ-L4, radula. (D)—IZ-L4, posterior radular portion. (E)—IZ-L4, details of lateral tooth denticulation. (F)—IZ-T9, specimen 19 mm in length (preserved), posterior radular portion. (G)—IZ-N42, specimen 17 mm in length (preserved), posterior radular portion. (H)—IZ-N42, rachidian tooth. Abbreviations: sd—secondary denticles on outer side of lateral tooth. Scale bars: (A,C) = 200 μ m; (B,E) = 20 μ m; (D,F) = 50 μ m; (G,H) = 30 μ m.

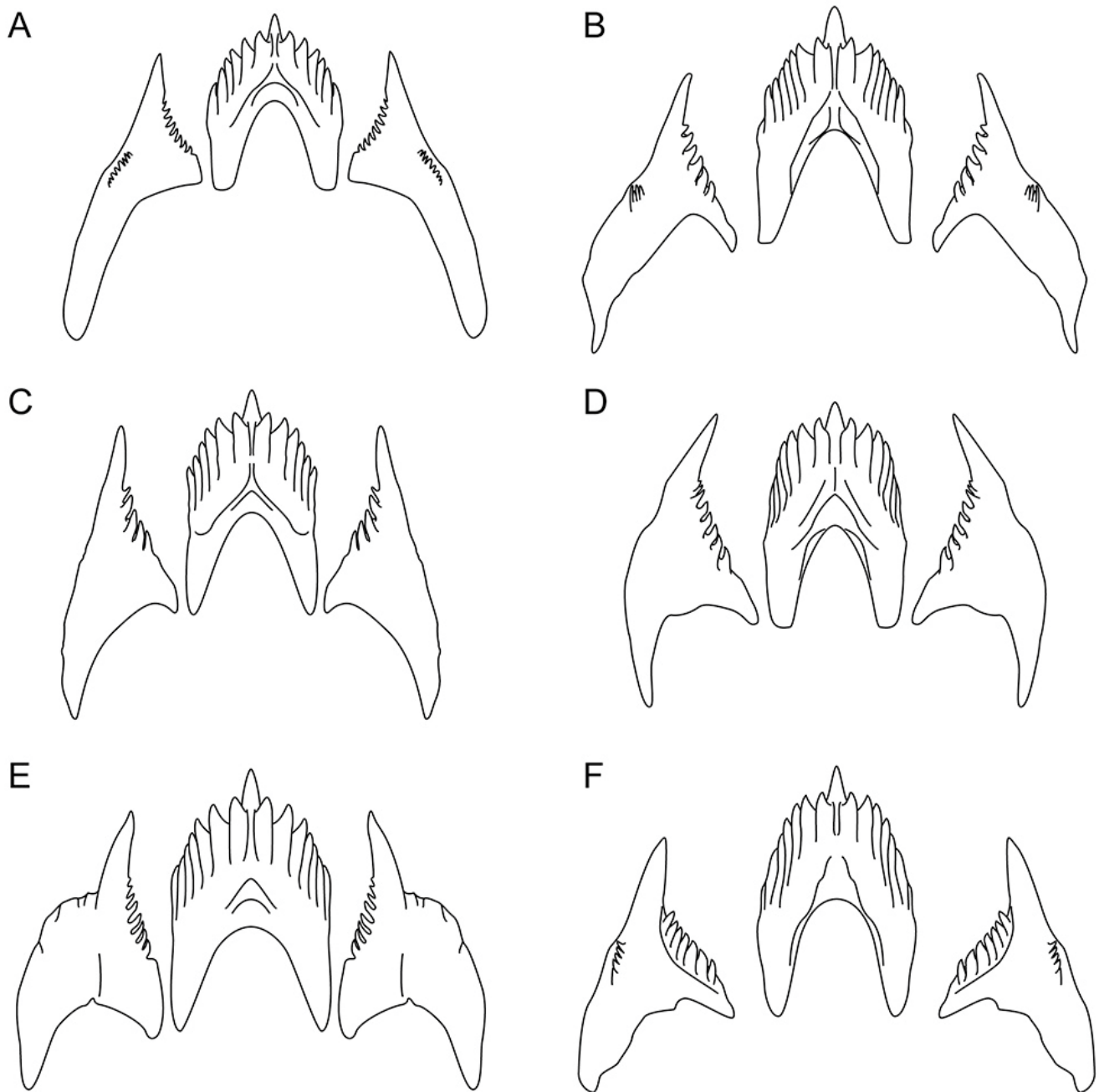


Figure 6. Diagrams of transverse radular row within *Coryphellina rubrolineata* species complex. (A)—*Coryphellina rubrolineata*. (B)—*Coryphellina lotos*. (C)—*Coryphellina pseudolotos* sp. nov. (D)—*Coryphellina pannaie* sp. nov. (E)—*Coryphellina flamma* sp. nov. (F)—*Coryphellina aurora* sp. nov.

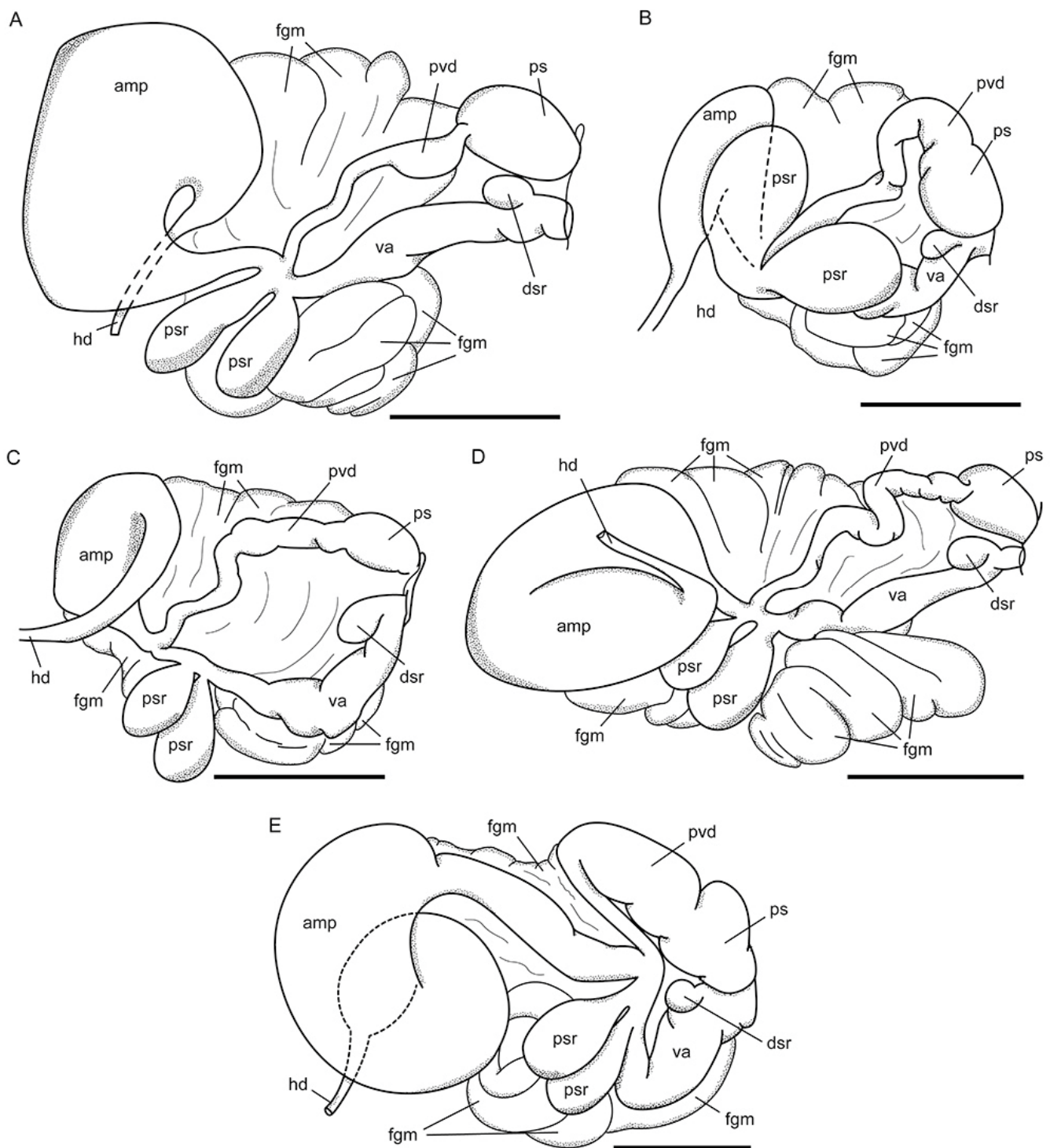


Figure 7. The reproductive system morphology in *Coryphellina rubrolineata* species complex. (A)—*Coryphellina lotos*. (B)—*Coryphellina pseudolotos* sp. nov. (C)—*Coryphellina pannaiae* sp. nov. (D)—*Coryphellina flamma* sp. nov. (E)—*Coryphellina aurora* sp. nov. Abbreviations: amp—ampulla; dsr—distal seminal receptaculum; fgm—female gland mass; hd—hermaphroditic duct; ps—penial sac; psr—proximal seminal receptaculum; pvd—prostatic vas deferens; va—vagina. Scale bars: (A,D,E) = 1 mm; B, C = 0.5 mm.

Distribution: Records of this species are confirmed in two localities: Pacific coast of Honshu, Japan (the type locality, Korshunova et al. [38]) and Central Vietnam (Nha Trang Bay: Hon Mun, Hon Mot, Hon Tre) (this study). It is likely that this species has a wide

distribution range in the Indo-West Pacific [40]; however, it must be verified by testing DNA samples.

Ecology: Found on stones and rocks on sandy bottom at 5–20 m in depth.

Genetic barcode: ON040918-ON040922.

Remarks: This species shows high variability in coloration, having white, pink, or violet chromatic variations (Figure 3). Discontinuous dorsal and dorsolateral pigmental lines are the main diagnostic traits. The dorsal line is often thick in the head region and poorly visible along the dorsum. In this trait, *C. lotos* differs from the rest of the genus diversity except for *C. pseudolotos* sp. nov. (see below). In addition, *C. lotos* has specific morphology of the lateral teeth, possessing large and long attenuated processes at their basal outer side, while in other species, these processes are much shorter (Figures 5 and 6B).

3.3.2. *Coryphellina pseudolotos* sp. nov.

Figures 4, 6C, 7B and 8

Zoobank lsid: urn:lsid:zoobank.org:act:D3502637-84EC-4CB9-8D89-4DE13C3B49F7

Type material: **Holotype:** ZIN63213, 15 mm in length preserved, Vietnam, Phu Quoc, st. 1, N 9°55'20.40" E 103°59'50.58", 10 m in depth, 27 April 2018, coll. E.S. Mekhova.

Paratypes: ZIN63214, 1 specimen, dissected, 7 mm in length preserved, Vietnam, Nha Trang, Hon Mot, N 12°10'27.56" E 109°16'19.61", 16–20 m in depth, on hydroids, 21 October 2016, coll. T.I. Antokhina. ZIN63215, 1 specimen, dissected, 12 mm in length preserved, Phu Quoc, st. 1, N 9°55'20.40" E 103°59'50.58", 10 m in depth, 27 April 2018, coll. E.S. Mekhova.

Type locality: Vietnam, Phu Quoc, N 9°55'20.40" E 103°59'50.58", 10 m in depth.

Additional material studied: IZ-N114, small damaged specimen, only DNA sample remained, Vietnam, Nha Trang, Hon Tre, N 12°10'54.95" E 109°17'37.94", 8 m in depth, on hydroids, 12 April 2017, coll. Y.V. Deart.

Etymology: The species name refers to the similarities of *C. pseudolotos* sp. nov. to *C. lotos* in external and internal morphology.

External morphology (Figure 8A–C): Length up to 15 mm (preserved). Body slender, foot slender with long anterior corners. Oral tentacles two times longer than rhinophores. Rhinophores highly papillated, bearing up to 50 papillae on inner side. Cerata finger-shaped, pointed distally, elongated, arranged in distinct groups on low elevations. Up to six groups of cerata per row. First group largest, with 9–12 cerata in group. Second group with 3–5 cerata. Cnidosacs on top of cerata. Digestive gland diverticula cylindrical, fill about 1/3–1/2 of ceratal volume. Well-defined discontinued notal edge under ceratal groups. Anus pleuroproctic. Reproductive openings lateral, below first group of cerata.

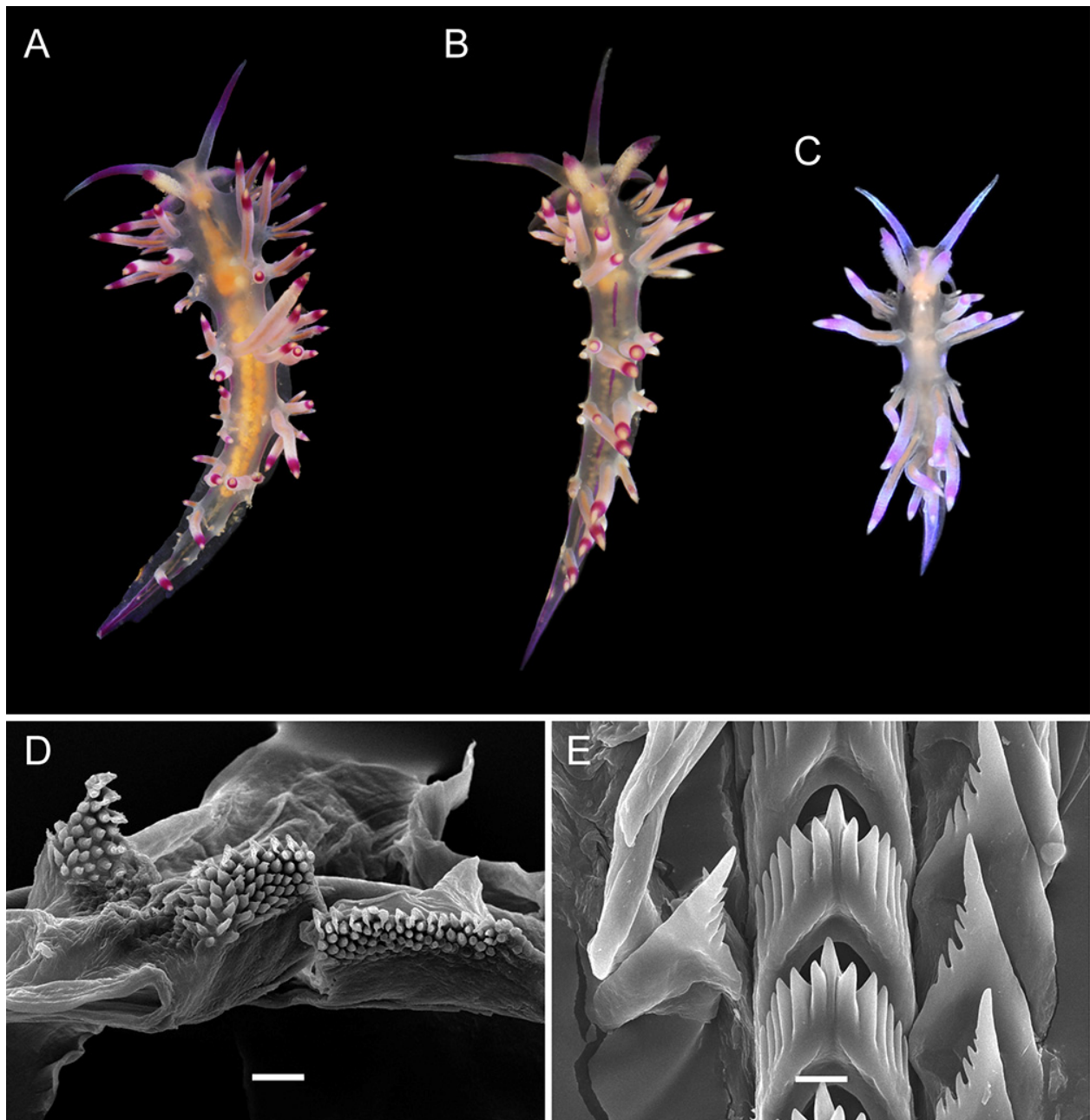


Figure 8. *Coryphellina pseudolotos* sp. nov., external morphology and buccal armature. (A)—holotype ZIN63213, specimen 15 mm in length (preserved). (B)—paratype ZIN63215, specimen 12 mm in length (preserved). (C)—paratype ZIN63214, specimen 7 mm in length (preserved). (D)—paratype ZIN63215, masticatory border of jaws. (E)—paratype ZIN63215, posterior radular portion. Scale bars: (D) = 20 μ m; (E) = 10 μ m. Photo credits: (A,B): Elena Mekhova; (C): Tatiana Antokhina.

Color (Figures 4 and 8A–C): Background color translucent. Digestive gland diverticula in cerata from peachy to light brown. Cerata translucent white, red to violet subapical rings with sparse white opalescent speckling underneath, white to peachy cnidosac area. Short pink to violet line between oral tentacles, line on body discontinuous in some specimens indistinct. Pink to violet discontinuous lines located laterally in ceratal intergroup space under notal edge, continuing from head to tail. Tail pink to violet. Rhinophores same color as body or light yellow, violet, or purple subapical rings. Oral tentacles pink to violet, more intensive in middle, white or translucent tip.

Internal morphology (Figures 6C, 7B and 8D,E): Jaws composed of two triangular plates with triangular masticatory process. Masticatory process with numerous sharp denticles, arranged in up to six rows, outermost denticles hamate with secondary dentitions at base, innermost sharp (Figure 8D). Radula triseriate, radular formula: 17–22 × 1.1.1 (Figure 8E). Rachidian tooth elongated-triangular with short conical central cusp, bearing six large denticles with deep furrows on both sides. Cusp sharp, small, slightly compressed by adjacent denticles. Lateral teeth narrow triangular with elongated cusp and 4–7 denticles on inner edge. Base of teeth with short attenuated processes. Small dentitions on outer tooth side absent. Reproductive system diaulic (Figure 7B). Ampulla large, sausage-shaped. Proximal seminal receptacle bilobed. Vas deferens slightly widens distally before entering penial sac, presenting prostatic area. Mucous gland lays distally into vagina, albumen and membrane glands next to proximal seminal receptacle. Their connection to vagina is not clear. Distal seminal receptacle small, opened into vagina distally. Penis small, conical, unarmed.

Distribution: The confirmed distributional range includes Southern (Phu Quoc Island) and Central (Nha Trang Bay: Hon Mot, Hon Tre) Vietnam. A specimen that is genetically similar to this species was collected in Queensland, Australia (GenBank COI accession: KJ001316), suggesting this species may have wider distribution.

Ecology: Found on stones and rocks on soft bottom at 5–20 m in depth.

Genetic barcode: ON040923-ON040925.

Remarks: This species closely match the morphology of its sibling species *C. lotos* (Figures 3, 4 and 8). Both species are found sympatrically in Central Vietnam (Nha Trang Bay: Hon Mot, Hon Tre). Nevertheless, the differences in nuclear marker 28S (one substitution in all studied specimens, 0.37%) and relatively high interspecific *p*-distance (9.63%) in mitochondrial COI indicate the existence of genetic barriers in these lineages. Therefore, we conclude that *C. pseudolotos* sp. nov. represents a distinct cryptic species. In morphological characters, the *C. pseudolotos* sp. nov. differs from *C. lotos* by the translucent coloration of the body that remains in an adult state (in specimens ~20 mm in length) (Figure 8A–C), while *C. lotos* is usually brightly colored with iridescent white to lilac background color (Figure 3). In addition, *C. pseudolotos* sp. nov. has a shorter process in lateral teeth and much fewer denticles than in *C. lotos* (Figure 6B,C). From other species of the *C. rubrolineata* species complex, the new species differs in the presence of three discontinuous red dorsal and dorsolateral lines (Table 2). Genetically it differs from them by 10.62–13.09% in COI, 0.43–4.29% in H3, and 1.48–12.18% in 28S (Table S3). We also detected a 4.20% *p*-distance in the COI marker between Vietnamese specimens and samples from Australia (GenBank data). It may be explained by either intraspecific variability across distant populations of a single species or by the presence of hidden cryptic diversity. To clarify this issue, more DNA-based studies of this complex in the Indo-West Pacific should be conducted.

Table 2. Comparative morphology of species within *Coryphellina rubrolineata* species complex. Abbreviations: OT = oral tentacles; RH—rhinophores; DG—digestive gland.

Trait	<i>C. rubrolineata</i> O'Donoghue, 1929	<i>C. lotos</i> Korshunova et al., 2017	<i>C. pseudolotos</i> sp. nov.	<i>C. panna</i> sp. nov.	<i>C. flamma</i> sp. nov.	<i>C. aurora</i> sp. nov.
Maximal length	12 mm	23 mm (preserved)	15 mm (preserved)	6 mm (preserved)	13 mm (preserved)	27 mm (preserved)
OT vs. RH length	2–3 times longer	1.5–2	2	1.5–2	1.5	1.2–1.5
Groups of cerata	Up to 7	6	6	5	5–7	9
Cerata in first group	8–12	9–13	9–12	8–9	8–10	Up to 23
Cerata in second group	5	4–5	3–5	3	5	7
DG volume in cerata	1/2–1/3	1/3–1/4	1/3–1/2	1/2	1/2–1/3	1/4–1/5

Table 2. Cont.

Trait	<i>C. rubrolineata</i> O'Donoghue, 1929	<i>C. lotos</i> Korshunova et al., 2017	<i>C. pseudolotos</i> sp. nov.	<i>C. panna</i> sp. nov.	<i>C. flamma</i> sp. nov.	<i>C. aurora</i> sp. nov.
Background color	Translucent to milky-white	Translucent white to purple	Translucent	Translucent white to light lilac	Translucent white with opaque white patches on ceratal groups	Translucent violet
OT color	White opalescent powder with lilac subapical rings	White to purple with intensive pink to purple subapical ring, translucent tip	Pink to violet, more intensive in middle, white or translucent tip	Translucent violet more intensive to tip, white tips	White opalescent powder with lilac subapical rings and translucent tips	Translucent violet more intensive to tip, white tips
Rhinophores color	Lilac tips and light-orange patches underneath them	Same color as body or apricot, purple subapical rings	Same color as body or light yellow, violet or purple subapical rings	Light pink, purple subapical rings, white tips	Translucent white, orange papillae, violet-red subapical rings	Intensive pink with orange papillae
Cerata color	White to violet, orange pigment on cnidosac area, purple subapical rings	Peachy to purple, red to violet subapical rings, peachy cnidosac area	Translucent white to peachy, red to violet subapical rings, white to peachy cnidosac area	Milky-white, white to yellow cnidosac area, red subapical rings	Two rings of salmon pink and peachy orange or brown, light-pink tips	Pink to lilac, violet-red subapical rings, peachy tips
Dorsal line	Continuous, purple, thickened on head and tail	Discontinuous, pink, thickened on head, on body indistinct	Discontinuous, pink, on body indistinct	Continuous, pink	Continuous to 2/3 of body length, then discontinuous, pink	Only on head, indistinct
Dorsolateral lines	Continuous, purple	Discontinuous, lilac	Discontinuous, lilac	Continuous, pink	Continuous, pink	Absent
Jaw masticatory border	8 rows	5 rows	6 rows	4 rows	7 rows	10 rows
Rows of teeth (radula)	27–34	27–35	17–22	15	23–25	36
Denticles on rachidian tooth (one side)	5–8	5–7	6	6–7	6–9	6–7
Denticles on laterals	8–11	8–11	4–7	7–9	8–12	7–8
Ampulla	Sausage-shaped	Sausage-shaped, widened in middle	Large, sausage-shaped	Large, sausage-shaped	Sausage-shaped, bent in midline	Sausage-shaped, coiled
Prostatic vas deference	With loops	Slightly widens	Slightly widens	With loops	Gradually widens	narrow Proximally, bent and expanded distally

3.3.3. *Coryphellina panna* sp. nov.

(Figures 4, 6D, 7C and 9)

Zoobank lsid: urn:lsid:zoobank.org:act:F42B143B-B8F1-4659-A1BD-412DAFC98C8F

Type material: **Holotype**: ZIN63216, 6 mm in length preserved, Vietnam, Nha Trang, Dambay, N 12°11'44.20" E 109°17'28.03", 5 m in depth, 16 April 2017, coll. Y.V. Deart. **Para-type**: ZIN63217, dissected, 5 mm in length preserved, Vietnam, Nha Trang, Dambay, N 12°11'39.84" E 109°17'26.74", 5 m in depth, 25 April 2018, coll. Y.V. Deart.

Type locality: Vietnam, Nha Trang, Tre Is., Dambay station, N 12°11'44.20" E 109°17'28.03", 5 m depth.

Etymology: Named after Panna I. Ekimova, mother of the first author.

External morphology (Figure 9A–C): Length up to 6 mm (preserved). Body slender, foot slender with long anterior corners. Oral tentacles 1.5–2 times longer than rhinophores.

Rhinophores highly papillated, bearing up to 40 papillae on inner side. Cerata finger-shaped, pointed distally, elongated, arranged in distinct groups. Up to five groups of cerata per row. First group largest, with 8–9 cerata in group. Second group with three cerata. Cnidosacs on top of cerata. Digestive gland diverticula cylindrical, fill about $\frac{1}{2}$ of ceratal volume. Well-defined discontinued notal edge under ceratal groups. Anus pleuroproctic. Reproductive openings lateral, below first group of cerata.

Color (Figures 4 and 9A–C): Background from translucent white to light lilac. Digestive gland diverticula in cerata from white to light yellow. Cerata milky-white, white to yellow cnidosac area with red subapical rings. Prominent dorsal pink line beginning between oral tentacles and continuing to tail. Two pink pigmental lines located laterally under notal edge, continuing from head to tail. All three lines merging on dorsal side of tail. Rhinophores light pink, purple subapical rings, white tips. Oral tentacles translucent violet, more intensive to tip, tips white.

Internal morphology (Figures 6D, 7C and 9D–F): Jaws composed of two triangular plates with triangular masticatory process. Masticatory process with numerous sharp denticles, arranged in up to four rows. Radula triseriate, radular formula: $15 \times 1.1.1$ (Figure 9D–F). Rachidian tooth elongated-triangular with short conical central cusp, bearing 6–7 large denticles with deep furrows on both sides. Cusp sharp, small, slightly compressed by adjacent denticles. Lateral teeth triangular, slightly curved, with elongated cusp and 7–9 denticles on inner edge. Base of teeth with short attenuated processes. Small dentitions on outer tooth side absent. Reproductive system diaulic (Figure 7C). Ampulla large, sausage-shaped. Proximal seminal receptacle bilobed. Vas deferens loops and widens distally before entering penial sac, presenting prostatic area. Mucous gland lays distally into vagina, albumen, and membrane glands next to proximal seminal receptacle. Their connection to vagina is not clear. Distal seminal receptacle small, opened into vagina distally. Penis small, conical, unarmed.

Distribution: This species is known only from the type locality.

Ecology: Both specimens were found on artificial substrate (old net) on sandy bottom at 5 m in depth. This species likely prefers sheltered environment.

Genetic barcode: ON040926, ON040927.

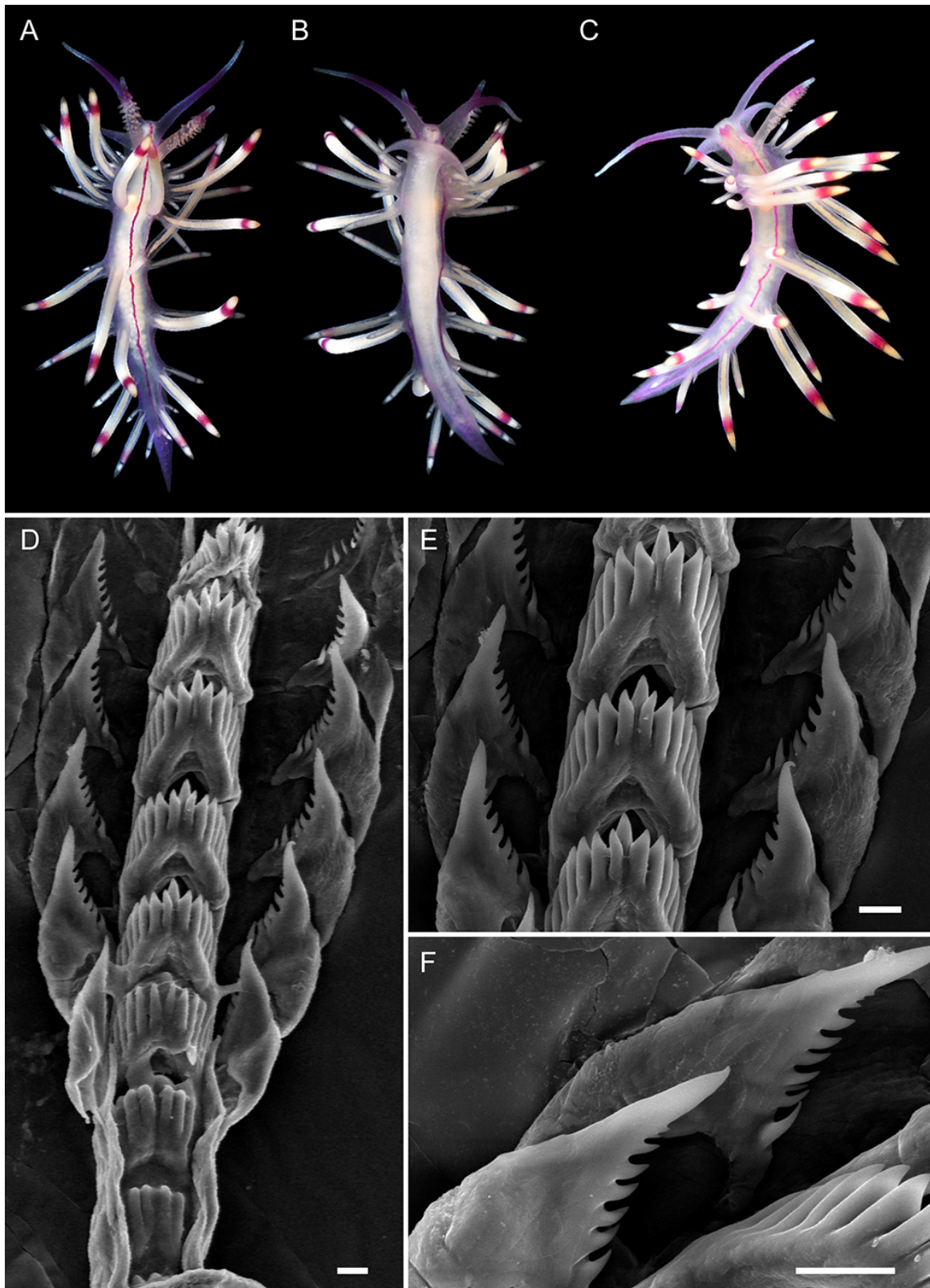


Figure 9. *Coryphellina pannae* sp. nov., external morphology and buccal armature. (A)—paratype ZIN63217, specimen 5 mm in length (preserved), dorsal view. (B)—paratype ZIN63217, ventral view. (C)—holotype ZIN63216, specimen 6 mm in length (preserved), dorsal view. (D)—paratype ZIN63217, posterior radular portion. (E)—paratype ZIN63217, rachidian and lateral teeth. (F)—paratype ZIN63217, lateral teeth. Scale bars: 10 μ m. Photo credit: (A–C): Yury Deart.

Remarks: The results of morphological and molecular analyses support *C. pannae* sp. nov. to be a new distinct species. Genetically it differs from the rest of the *C. rubrolineata* species complex diversity by 10.62–15.31% in COI, 2.15–3.86% in H3, and 4.80–12.55% in 28S (Table S3). Morphologically it differs from the rest diversity of the *C. rubrolineata* species complex by smaller body size (up to 6 mm in adult state, preserved specimen), presence of three continuous lines, white coloration of body, low number of cerata, and triangular curved form of the lateral teeth (Table 2). In coloration pattern, the new species is most similar to the *C. rubrolineata* (Figures 4 and 9); however, the latter species is usually covered by white opalescent powder [39], while *C. pannae* sp. nov. is translucent white to light lilac. In addition, *C. rubrolineata* has more cerata in each group, and more groups of cerata (up to 7 in *C. rubrolineata* and 5 in *C. pannae* sp. nov.) (Table 2).

3.3.4. *Coryphellina flamma* sp. nov.

(Figures 4, 6E, 7D, 10 and 11)

Zoobank lsid: urn:lsid:zoobank.org:act:4A89825D-ED98-40B9-9AE2-5C4CDC44060C

Type material: **Holotype:** ZIN63218, 12 mm in length preserved, Vietnam, Nha Trang, Hon Nok, N 12°11'23.17" E 109°20'40.87", 10 m in depth, 12 July 2019, coll. Y.V. Deart.

Paratypes: ZIN63219, 1 specimen, dissected, 10 mm in length preserved, Vietnam, Tho Chu, st. 5, N 9°15'25.74" E 103°28'10.08", 8–10 m in depth, 10 May 2018, coll. E.S. Mekhova.

ZIN63220, 1 specimen, damaged during collection, 13 mm in length preserved, Vietnam, Nha Trang, Hon Nok, N 12°11'23.17" E 109°20'40.87", 10 m in depth, 12 July 2019, coll. Y.V. Deart.

ZIN63221, 1 specimen, dissected, 12 mm in length preserved, Vietnam, Nha Trang, Hon Nok, N 12°11'23.17" E 109°20'40.87", 10 m in depth, 12 July 2019, coll. Y.V. Deart.

ZIN63222, 3 specimens, 2 dissected, 7–12 mm in length preserved, Vietnam, Nha Trang, Hon Nok, N 12°11' E109°20', depth unknown, 22 April 2019, coll. E.S. Mekhova.

ZIN63223, 1 specimen, dissected, 10 mm in length preserved, Vietnam, Nha Trang, Hon Nok, N 12°11'27.74" E 109°20'31.16", 12 m in depth, on rocks, 10 June 2021, coll. Y.V. Deart.

Type locality: Vietnam, Nha Trang, Hon Nok, N 12°11'22.29" E 109°20'43.14", 10 m depth.

Etymology: from *flamma* (= flame, fire, Latin), referring to reddish-orange coloration of this species.

External morphology (Figure 10): Length up to 13 mm (preserved). Body slender, foot slender with long anterior corners. Oral tentacles 1.5 times longer than rhinophores. Rhinophores highly papillated, bearing up to 50 papillae on inner side. Cerata finger-shaped, pointed distally, elongated, arranged in distinct groups. Up to seven groups of cerata per row. First group largest, with 8–10 cerata in group. Second group with five cerata. Cnido-sacs on top of cerata. Digestive gland diverticula cylindrical, fill about 1/2–1/3 of ceratal volume. Well-defined discontinued notal edge under ceratal groups. Anus pleuroproct. Reproductive openings lateral, below first group of cerata.

Color (Figures 4 and 10): Background translucent white with opaque-white opalescent patches below ceratal groups on dorsum and lateral sides. Digestive gland diverticula in cerata brownish. Cerata with two rings of salmon pink pigmentation alternating with peachy orange or reddish-brown, tips light pink. Prominent thick pink line on dorsal midline, thickened between oral tentacles, narrowing and becoming discontinuous at posterior dorsum part. Two other pink pigment lines located laterally under notal edge, continuing from head to tail. All three lines merging on dorsal side of tail. Rhinophores translucent white with orange papillae, violet-red subapical rings and translucent tips. Oral tentacles covered by sparse white opalescent powder with lilac subapical rings and translucent tips.

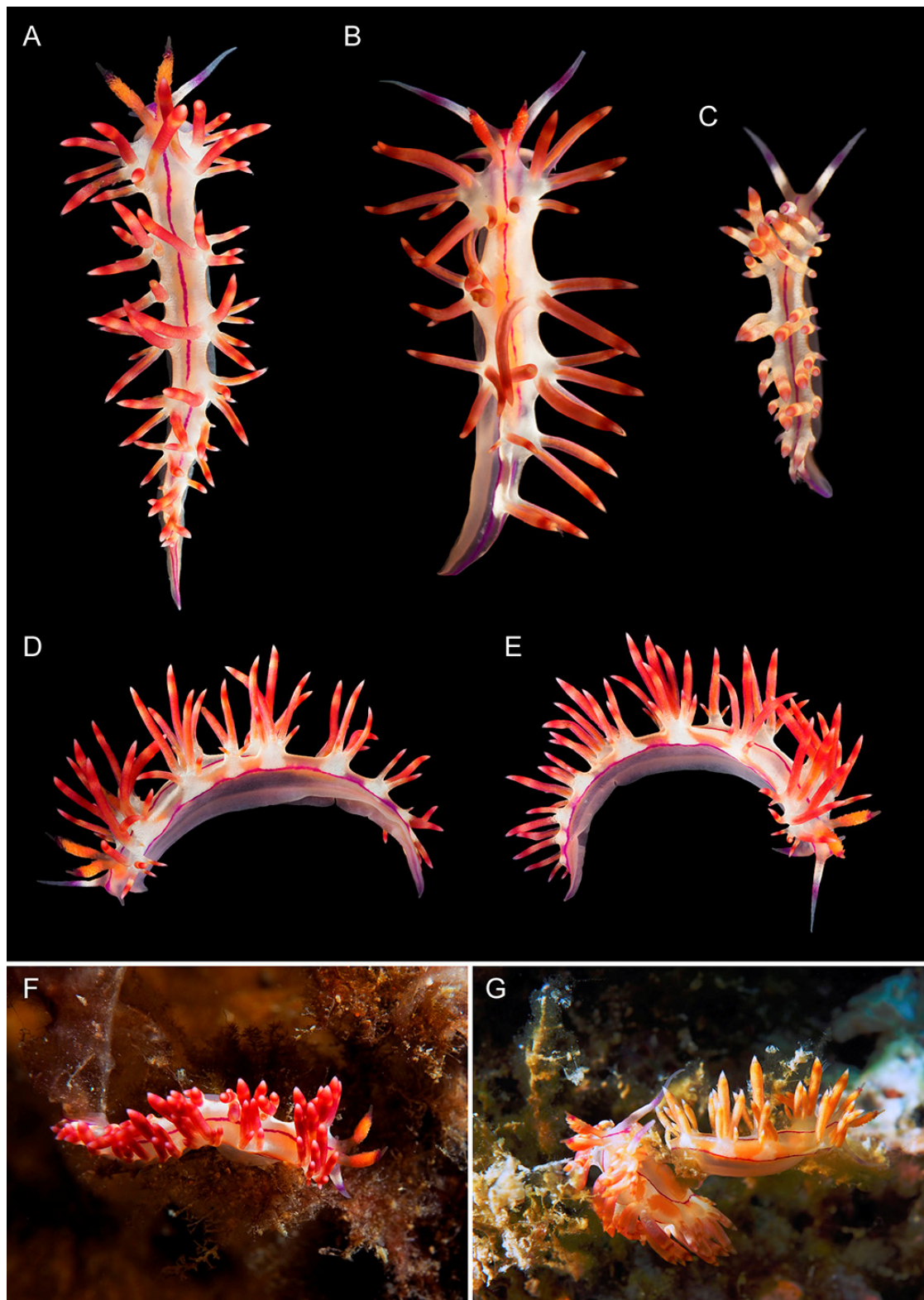


Figure 10. *Coryphellina flamma* sp. nov., external morphology. (A)—holotype ZIN63218, specimen 12 mm in length (preserved), dorsal view. (B)—paratype ZIN63219, specimen 10 mm in length (preserved). (C)—paratype ZIN63222, specimen 7 mm in length (preserved). (D)—holotype ZIN63218, lateral view from left. (E)—holotype ZIN63218, lateral view from right. (F)—holotype ZIN63218 in natural environment. (G)—paratypes ZIN63220, ZIN63221 in natural environment. Photo credits: (A,D–G): Yury Deart; (B,C): Elena Mekhova.

Internal morphology (Figures 6E, 7D and 11): Jaws composed of two triangular plates with triangular masticatory process (Figure 11A). Masticatory process with numerous sharp denticles, arranged in up to six rows (Figure 11B,C). Radula triseriate, radular formula: 23–25 × 1.1.1 (Figure 11D–I). Rachidian tooth triangular with short conical central cusp, bearing 6–9 large denticles with deep furrows on both sides. Cusp sharp, small, slightly compressed by adjacent denticles. Lateral teeth triangular with elongated cusp and 8–12 denticles on inner edge. Teeth slightly curved distally, with short attenuated processes. Dentitions on outer tooth side absent. Reproductive system diaulic (Figure 7D). Ampulla large, sausage-shaped, bent in midline. Proximal seminal receptacle bilobed. Vas deferens gradually widens distally before entering penial sac, presenting prostatic area. Mucous gland lays distally into vagina, albumen, and membrane glands next to proximal seminal receptacle. Their connection to vagina is not clear. Distal seminal receptacle small, opened into vagina distally. Penis small, conical, unarmed.

Distribution: For now, this species is known only from Central (Nha Trang: Hon Nok), and Southern (Tho Chu Is.) Vietnam. Probably it has a wider distribution in the Indo-West Pacific.

Ecology: Found on hydroids on rocks and vertical walls in exposed conditions on 5–15 m in depth.

Genetic barcode: ON040929-ON040933.

Remarks: The results of morphological and molecular analyses support *C. flamma* sp. nov. to be a new distinct species. Genetically it differs from the rest of the *C. rubrolineata* species complex diversity by 9.38–15.31% in COI, 1.72–4.29% in H3, and 1.85–11.44% in 28S (Table S3). In external characters, this species differs from other representatives of the *C. rubrolineata* species complex in the presence of three continuous red lines on dorsal and dorsolateral sides and a peculiar orange-red to bright-red coloration pattern with orange rhinophores and opaque-white pigmental patches on the notal edge below cerata (Table 2). *Coryphellina pannae* sp. nov. and *C. rubrolineata* also have three continuous lines but differ in coloration pattern (see above and Ekimova et al. [39]) by overall whitish background color and white to lilac cerata.

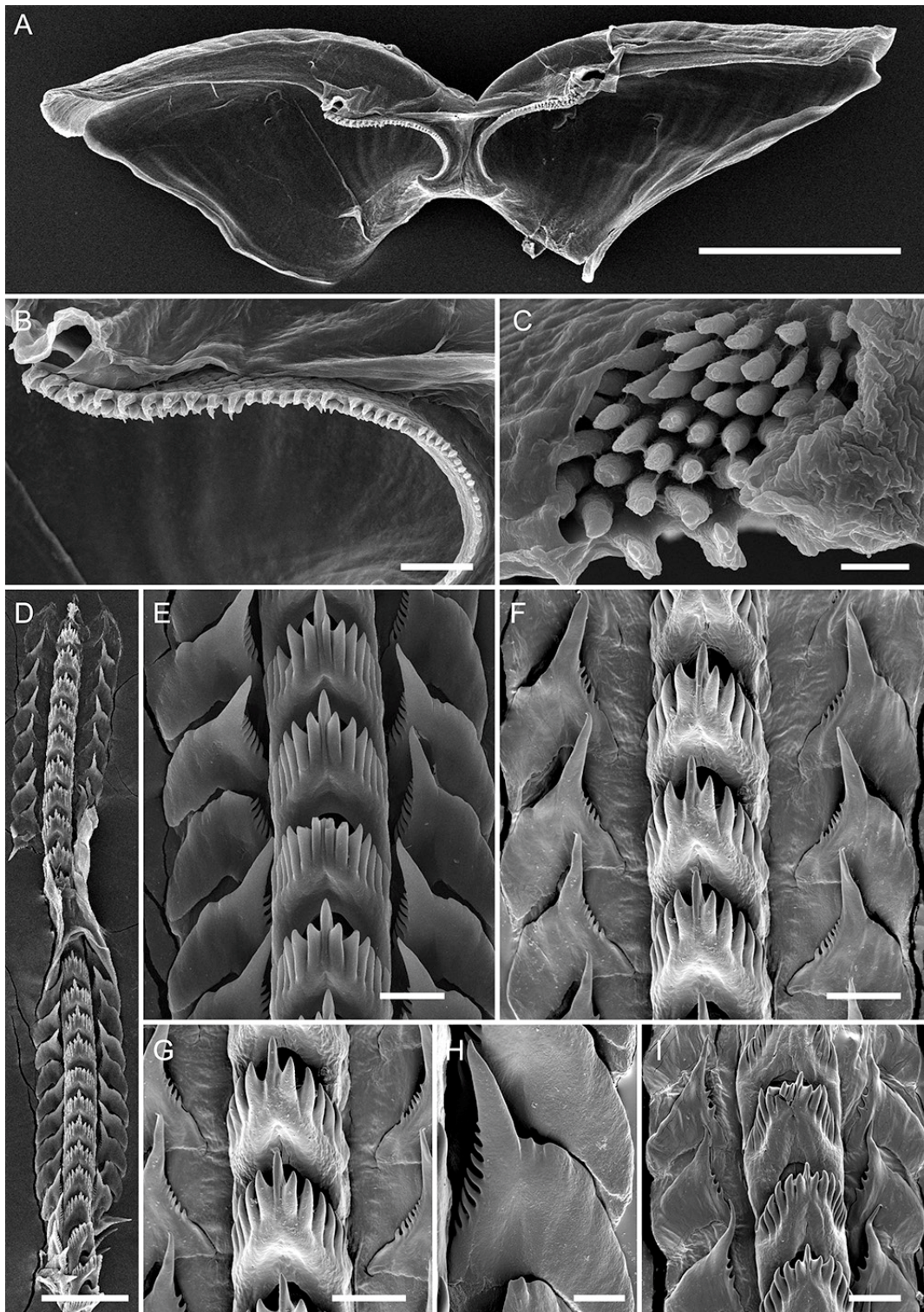


Figure 11. *Coryphellina flamma* sp. nov., buccal armature. (A)—Paratype ZIN63219, jaw plates. (B)—paratype ZIN63219, masticatory process. (C)—paratype ZIN63222, denticulation of masticatory border. (D)—paratype ZIN63222 (specimen 12 mm in length), radula. (E)—paratype ZIN63222 (specimen 12 mm in length), anterior radular portion. (F)—paratype ZIN63222 (specimen 12 mm in length), posterior radular portion. (G)—paratype ZIN63222 (specimen 12 mm in length), rachidian teeth. (H)—paratype ZIN63222 (specimen 12 mm in length), lateral tooth. (I)—paratype ZIN63222 (specimen 7 mm in length), posterior radular portion. Scale bars: (A) = 500 μ m; (B) = 50 μ m; (C,H) = 10 μ m; (D) = 100 μ m; (E–G, I) = 20 μ m.

3.3.5. *Coryphellina aurora* sp. nov.

(Figures 4, 6F, 7E, 12 and 13)

Zoobank lsid: urn:lsid:zoobank.org:act:FCAB9741-416D-4994-83EF-5DF2A9BB5AC6

Type material: **Holotype** ZIN63224, 27 mm in length preserved, specimen dissected, radula and jaws mounted on aluminum stub, Vietnam, Nha Trang, Hon Nok, N 12° 11' 22.29" E 109° 20' 43.14", 25 m depth, collected 25 July 2019, coll. Y.V. Deart.

Type locality: Vietnam, Nha Trang, Hon Nok, N 12° 11' 22.29" E 109° 20' 43.14", 25 m depth.

Etymology: From *aurora* (= dawn, Latin) referred to the beautiful pinkish coloration of this species, resembling the color patterns of the sunrise along the Vietnamese coast.

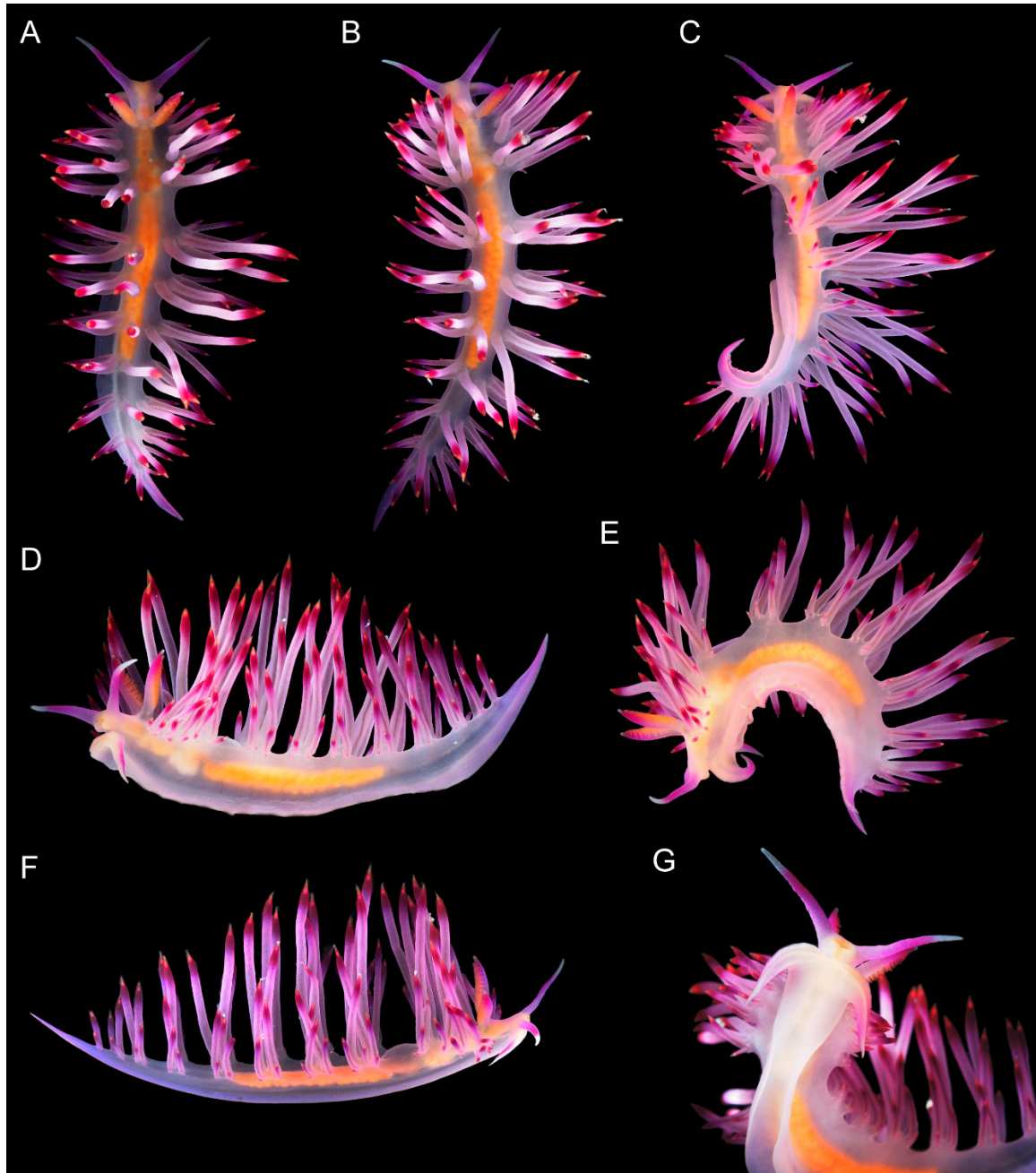


Figure 12. *Coryphellina aurora* sp. nov., holotype ZIN63224, specimen 27 mm in length (preserved), external morphology. (A–C)—dorsal view. (D,E)—lateral view from left. (F)—lateral view from right. (G)—ventral view on anterior body part. Photo credit: Yury Deart.

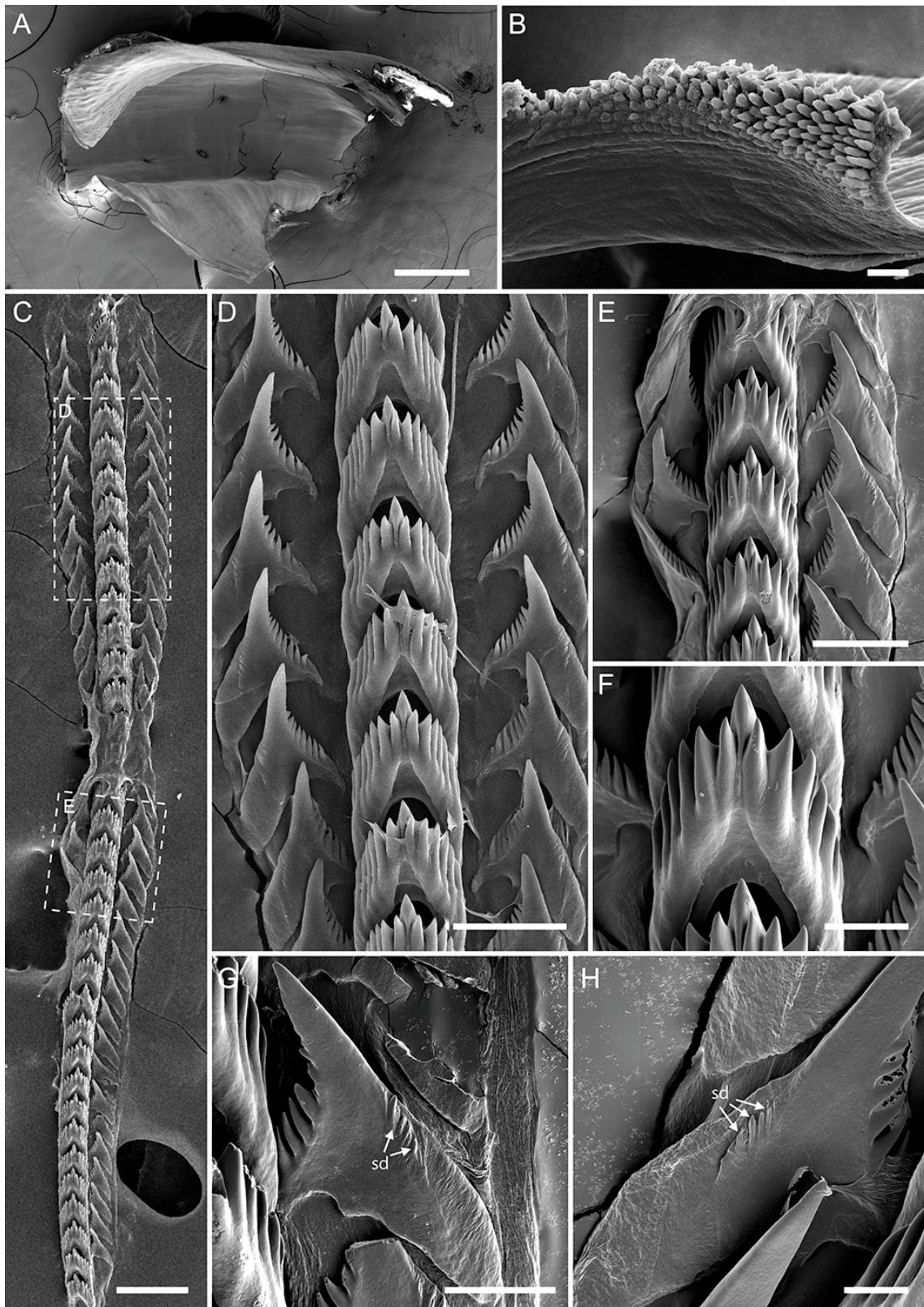


Figure 13. *Coryphellina aurora* sp. nov., holotype ZIN63224, buccal armature. (A)—left jaw plate. (B)—denticulation of masticatory process. (C)—radula. (D)—posterior radular portion. (E)—middle radular portion. (F)—rachidian tooth. (G)—lateral tooth. (H)—lateral tooth. Abbreviations: sd—secondary denticles on outer side of lateral tooth. Scale bars: (A,C) = 200 μm ; (B,E) = 20 μm ; (D,F) = 50 μm ; (G,H) = 30 μm .

External morphology (Figure 12): Length up to 27 mm (preserved). Body slender, foot slender with long anterior corners. Oral tentacles 1.2–1.5 times longer than rhinophores. Rhinophores highly papillated, bearing up to 70 papillae on inner side. Cerata cylindrical, pointed distally, elongated, arranged in distinct groups. Up to nine groups of cerata per row. First group largest, with up to 23 cerata in group. Second group with seven cerata. Cnidosacs on top of cerata. Digestive gland diverticula cylindrical, fill about 1/4–1/5 of ceratal volume. Well-defined discontinued notal edge under ceratal groups. Anus pleuroproctic. Reproductive openings lateral, below first group of cerata.

Color (Figures 4 and 12): Background translucent violet. Digestive gland diverticula in cerata brownish. Cerata pink to lilac, violet-red subapical rings with sparse white opalescent speckling underneath and orange tips. Indistinct short pink dorsal line on head. Rhinophores intensive pink with orange papillae and translucent tips. Oral tentacles translucent violet to pink more intensive to tip, tips covered by sparse white opalescent powder.

Internal morphology (Figures 6F, 7E and 13): Jaws composed of two triangular plates with triangular masticatory process (Figure 13A). Masticatory process with numerous sharp denticles, arranged in up to 10 rows, outermost denticles hamate with secondary dentitions at base, innermost sharp (Figure 13B). Radula triseriate, radular formula: $36 \times 1.1.1$. Rachidian tooth elongated-triangular with short conical central cusp, bearing 6–7 large denticles with deep furrows on both sides. Cusp sharp, small, slightly compressed by adjacent denticles. Lateral teeth triangular with elongated cusp and 7–8 denticles on inner edge. Base of teeth slightly curved proximally, oblong distally, with short attenuated processes. Small dentitions on outer tooth side (Figure 13G,H). Reproductive system diaulic (Figure 7E). Ampulla large and muscular, sausage-shaped, coiled. Proximal seminal receptacle bilobed. Vas deferens narrow proximally than bent and expanded into widened prostatic part. Mucous gland of amorphous structure, laying distally to vagina, albumen, and membrane glands next to proximal seminal receptacle, well developed. Their connection to vagina is not clear. Distal seminal receptacle small, opened into vagina dorsally. Penis small, conical, unarmed.

Distribution: For now, this species is known only from the type locality. Possibly this species is the same as *Flabellina* sp. 2 *sensu* Gosliner et al. [40], and therefore, its distribution may also include at least the Philippines.

Ecology: A single large specimen was found at 25 m in depth on rock.

Genetic barcode: ON040934.

Remarks: According to morphological and molecular data, *C. aurora* sp. nov. clearly represents a new distinct species. Genetically it differs from the rest of the *C. rubrolineata* species complex diversity by 11.60–16.30% in COI, 2.15–4.72% in H3, and 3.32–11.81% in 28S (Table S3). Morphologically its main diagnostic trait is the almost complete absence of dorsal and dorsolateral pigmental lines on the body (Figures 4 and 12). A single short and thin pink line presents only on the head between rhinophores. In addition, its peculiar pink to violet and lilac coloration serves as a suitable diagnostic trait for further identification of this species. In other external characteristics, this species is unique in the high number of ceratal groups (9) and in the high number of cerata in the first group (up to 23) (Table 2). In internal characters, *C. aurora* sp. nov. possesses up to 10 rows of denticles on the jaw masticatory border and has the longest radula among other species of the complex (36 rows of teeth) (Figure 13).

4. Discussion

Our results clearly show a much higher diversity in the genus *Coryphellina* than was previously suggested. All studied species conform to the diagnosis of the genus *Coryphellina* having papillate rhinophores, discontinuous notal edge, cerata arranged in groups, and bilobed proximal seminal receptaculum. These features clearly distinguish the genus *Coryphellina* from the representatives of the most closely related genus *Edmundsella* (includes *E. pedata* (Montagu, 1816) and *E. albomaculata* (Pola et al., 2014) see Korshunova et al. [38]) and representatives of the genus *Flabellina* (includes at least *Flabellina affinis* (Gmelin, 1791)), but clearly needs further revision, see Furfaro et al. [45]). The genus *Edmundsella* pos-

sesses smooth rhinophores, non-stalked cerata on elevations, and non-bilobed seminal receptaculum [38], while in *Flabellina s.str.*, rhinophores are annulated, cerata are placed on peduncles, and the seminal receptaculum is also simple [38,45,69]. It should also be mentioned that other genera (e.g., *Caronella*, *Calmella*, etc., see Korshunova et al. [38]) from the same clade as the *Flabellina s.str.* also have cerata on peduncles and rhinophores of different morphology, and thus they do not conform to the diagnosis of *Coryphellina* as well [38,45,69]. Therefore, our results strongly correspond to the taxonomical decision suggested by Korshunova et al. [38] and support the genus *Coryphellina* as a valid distinct taxon.

Our results indicate that the cryptic diversity found within the *Coryphellina* rubrolineata species complex is a pseudocryptic one in most cases, which means that morphological differences could be found with known genetic species boundaries. In this case, the main differences between species were found in the external morphology, i.e., coloration pattern (Figure 4), number of ceratal groups, and number of cerata per group (Table 2). In the coloration pattern, the most important trait is the extent of pigmental dorsal and dorso-lateral lines on the body. Only a thin dorsal midline remains between the rhinophores of *C. aurora* sp. nov. (Figure 12). In *C. lotos* and *C. pseudolotos* sp. nov., all three lines are usually present, but they are discontinuous, and the dorsal line is well developed only between the rhinophores (Figures 3 and 8A–C). Only in the *C. flamma* sp. nov., *C. panna*e sp. nov., and the “true” *C. rubrolineata* all three lines are well developed and continue along the whole body (Figures 9 and 10). The general coloration pattern is also an important distinctive trait, as *C. flamma* sp. nov. differs well from *C. panna*e sp. nov. by orange to red coloration of cerata and distinct white patches underneath groups of cerata, while *C. panna*e has translucent-white coloration (Figures 9 and 10). *Coryphellina lotos* usually demonstrates iridescent pinkish to violet coloration (Figure 3), while in its sister species, *C. pseudolotos* sp. nov., the general color of the body is translucent even in adult specimens (Figure 8A–C). Several differences may be found in radular characters and the morphology of the reproductive system (Table 2, Figure 7), but it is not clear whether these differences relate to animals’ size or maturity. Species complexes in which pseudocryptic species are differentiated mainly at a base of coloration pattern are well known in nudibranch research: the same was shown for the representatives of the genera *Pteraeolidia* [70], *Unidentia* [71], *Glossodoris*, *Doriprismatica* [72], and *Goniobranchus* [73].

From the biogeographical viewpoint, for now, three species are endemics to Vietnam waters: *C. panna*e sp. nov., *C. flamma* sp. nov., and *C. aurora* sp. nov. At the same time, specimens with similar coloration to *C. flamma* sp. nov. were recorded in other regions of the Indo-West Pacific, including the Philippines [28], Great Barrier Reef, Australia [74] and New Caledonia [75]. The same is true for the *C. aurora* sp. nov., as specimens of the same coloration pattern were listed as *Flabellina* sp. 2 collected in the Philippines [40]. Additional molecular studies are needed to confirm the wide distribution range of these species. In the case of *C. lotos* and *C. pseudolotos* sp. nov., the biogeographical implications are much more complex. *Coryphellina lotos* was initially described in temperate waters of Japan (Hokkaido) [38], and its specimens from Vietnam are very similar genetically but differ in general coloration of the body as most of the studied samples have a non-typical violet iridescent coloration. At the same time, its sister species, *C. pseudolotos* sp. nov., also possesses similar external morphological traits, while found differences in internal morphology are not obvious since they could be a result of ontogenetic variability. *Coryphellina pseudolotos* sp. nov. demonstrates low but stable differences in nuclear loci (the *p*-distance in the 28S marker is 0.37%), which suggests the restriction of gene flow between this species and sympatric *C. lotos* and supports the distinct status of the two species. In addition, a specimen, which is genetically similar to *C. pseudolotos* sp. nov., was collected in Australia [76]. However its taxonomical status is unclear due to the results of the species delimitation analyses (Figure 2), and since the morphological data are unavailable. Possibly, both *C. lotos* and *C. pseudolotos* sp. nov. have a wide distribution in the tropical Indo-West Pacific either in its northern (*C. lotos*) or southern (*C. pseudolotos* sp. nov.) parts, and the

Vietnamese waters are an area of their secondary sympatry. This hypothesis, as well as the identity of Australian specimens, should be tested in further integrative works on this species complex.

Supplementary Materials: The following are available online at <https://www.mdpi.com/article/10.3390/d14040294/s1>, Data S1: Unedited maximum likelihood trees based on single-gene data sets and the partitioned data set in NEWICK format; File Table S1: List of specimens used in this study, including voucher and field numbers, collection data, and collectors; File Table S2: Specimens used for molecular analysis. Voucher numbers, collection localities, and GenBank accession. Figure S1: The ASAP analysis; Figure S2: The same 11 candidate species were identified in the bPTP; Figure S3: GMYC analyses.

Author Contributions: Conceptualization, I.E.; methodology, I.E. and D.S.; software, D.S.; validation, I.E. and D.S.; formal analysis, I.E., Y.D., T.A., A.M. and D.S.; resources, I.E.; data curation, I.E. and Y.D.; writing—original draft preparation, I.E.; writing—review and editing, I.E., Y.D., T.A., A.M. and D.S.; visualization, I.E., Y.D., T.A. and A.M.; supervision, I.E.; project administration, I.E.; funding acquisition, I.E. All authors have read and agreed to the published version of the manuscript.

Funding: This study was carried out in the frame of a scientific project of the State Order of the Russian Federation Government to Lomonosov Moscow State University no. 122012100155-8 with the financial support of the Russian Science Foundation grant no. 20-74-10012.

Institutional Review Board Statement: Not applicable.

Informed Consent Statement: Not applicable.

Data Availability Statement: Unedited phylogenetic trees and results of species delimitation analyses are provided as Supplementary Material files. All sequences were deposited to GenBank.

Acknowledgments: We are deeply grateful to Elena Mekhova and Varvara Barkalova, who kindly collected and supplied additional specimens and their photos for this study. The authors gratefully acknowledge the Vietnamese-Russian Tropical Centre for the organization of field trips in Vietnam. We thank Maria Stanovova and Valentina Tambovtseva for their assistance with Sanger sequencing. Two anonymous reviewers and Academic Editors Giulia Furfaro and Paolo Mariottini are thanked for all corrections and suggestions, which helped to improve the initial version manuscript. The light microscopy and molecular studies were conducted using equipment of the Invertebrate Zoology Department MSU, the electron microscopy studies using equipment of the Electron Microscopy Laboratory of the Shared Facilities Center of Lomonosov Moscow State University sponsored by the Reuter Foundation Ministry of Education and Science and Joint Usage Center Instrumental methods in ecology at the IEE RAS. Sanger sequencing was conducted using equipment of the Core Centrum of the Institute of Developmental Biology RAS.

Conflicts of Interest: The authors declare no conflict of interest. The funders had no role in the design of the study, in the collection, analyses, or interpretation of data, in the writing of the manuscript, or in the decision to publish the results.

References

1. Knowlton, N. Sibling species in the sea. *Annu. Rev. Ecol. Syst.* **1993**, *24*, 189–216. [[CrossRef](#)]
2. Bickford, D.; Lohman, D.J.; Sodhi, N.S.; Ng, P.K.L.; Meier, R.; Winker, K.; Ingram, K.K.; Das, I. Cryptic species as a window on diversity and conservation. *Trends Ecol. Evol.* **2007**, *22*, 148–155. [[CrossRef](#)] [[PubMed](#)]
3. Ratnasingham, S.; Hebert, P.D.N. BOLD: The barcode of life data system (<http://www.barcodinglife.org>). *Mol. Ecol. Notes* **2007**, *7*, 355–364. [[CrossRef](#)] [[PubMed](#)]
4. Fauvel, P. Classes des annélides polychètes. Distribution géographique. *Trait. de Zool.* **1959**, *5*, 163–165.
5. Laakkonen, H.M.; Strelkov, P.; Väinölä, R. Molecular lineage diversity and inter oceanic biogeographical history in *Hiattella* (Mollusca, Bivalvia). *Zool. Scr.* **2015**, *44*, 383–402. [[CrossRef](#)]
6. Kienberger, K.; Carmona, L.; Pola, M.; Padula, V.; Gosliner, T.M.; Cervera, J.L. *Aeolidia papillosa* (Linnaeus, 1761) (Mollusca: Heterobranchia: Nudibranchia), single species or a cryptic species complex? A morphological and molecular study. *Zool. J. Linn. Soc. Lond.* **2016**, *177*, 481–506. [[CrossRef](#)]
7. Layton, K.K.; Martel, A.L.; Hebert, P.D. Geographic patterns of genetic diversity in two species complexes of Canadian marine bivalves. *J. Mollus. Stud.* **2016**, *82*, 282–291. [[CrossRef](#)]

8. McCarthy, J.B.; Krug, P.J.; Valdés, Á. Integrative systematics of *Placida cremoniana* (Trinchese, 1892) (Gastropoda, Heterobranchia, Sacoglossa) reveals multiple pseudocryptic species. *Mar. Biodivers.* **2019**, *49*, 357–371. [[CrossRef](#)]
9. Ekimova, I.; Valdés, Á.; Chichvarkhin, A.; Antokhina, T.; Lindsay, T.; Schepetov, D. Diet-driven ecological radiation and allopatric speciation result in high species diversity in a temperate-cold water marine genus *Dendronotus* (Gastropoda: Nudibranchia). *Mol. Phylogenet. Evol.* **2019**, *141*, 106609. [[CrossRef](#)]
10. Ekimova, I.A.; Mikhlina, A.L.; Vorobyeva, O.A.; Antokhina, T.I.; Tambovtseva, V.G.; Schepetov, D.M. Young but distinct: Description of *Eubranthus malakhovi* sp. n. a new, recently diverged nudibranch species (Gastropoda: Heterobranchia) from the Sea of Japan. *Invertbr. Zool.* **2021**, *18*, 197–222. [[CrossRef](#)]
11. Duran, S.; Rützler, K. Ecological speciation in a Caribbean marine sponge. *Mol. Phylogenet. Evol.* **2006**, *40*, 292–297. [[CrossRef](#)] [[PubMed](#)]
12. Churchill, C.K.; Valdés, Á.; Foighil, D.Ó. Molecular and morphological systematics of neustonic nudibranchs (Mollusca: Gastropoda: Glaucidae: Glaucus), with descriptions of three new cryptic species. *Invertebr. Syst.* **2014**, *28*, 174–195. [[CrossRef](#)]
13. Krug, P.J.; Vendetti, J.E.; Valdés, A. Molecular and morphological systematics of *Elysia* Risso, 1818 (Heterobranchia: Sacoglossa) from the Caribbean region. *Zootaxa* **2016**, *4148*, 1–137. [[CrossRef](#)] [[PubMed](#)]
14. Nygren, A.; Parapar, J.; Pons, J.; Meißner, K.; Bakken, T.; Kongsrud, J.A.; Oug, E.; Gaeva, D.; Sikorski, A.; Johansen, R.A.; et al. A mega-cryptic species complex hidden among one of the most common annelids in the North East Atlantic. *PLoS ONE* **2018**, *13*, e0198356. [[CrossRef](#)] [[PubMed](#)]
15. Krug, P.J. Patterns of speciation in marine gastropods: A review of the phylogenetic evidence for localized radiations in the sea. *Am. Malacol. Bull.* **2011**, *29*, 169–186. [[CrossRef](#)]
16. Fritts-Penniman, A.L.; Gosliner, T.M.; Mahardika, G.N.; Barber, P.H. Cryptic ecological and geographic diversification in coral-associated nudibranchs. *Mol. Phylogenet. Evol.* **2020**, *144*, 106698. [[CrossRef](#)]
17. O'Donoghue, C.H. Report on the Opisthobranchia. XXXVIII. Zoological results of the Cambridge Expedition to the Suez Canal. *Trans. Zool. Soc. Lon.* **1929**, *22*, 713–841.
18. Gat, G. *Flabellina rubrolineata* (O'Donoghue) and *Phidiana indica* (Bergh) (Nudibranchia: Aeolidoidea), two new Lessepsian immigrants in the Eastern Mediterranean. *J. Mollus. Stud.* **1993**, *59*, 120. [[CrossRef](#)]
19. Yokes, B.; Rudman, W.B. Lessepsian opisthobranchs from southwestern coast of Turkey: Five new records for Mediterranean. *Rapp. Comm. Int. Explor. Mer Méditerranée* **2004**, *37*, 557.
20. Yonow, N. Red Sea Opisthobranchia 4: The orders Cephalaspidea, Anaspidea, Notaspidea and Nudibranchia: Dendronotacea and Aeolidacea. *Fauna Arab.* **2000**, *18*, 87–132.
21. Yonow, N. Opisthobranchs of the Gulf of Eilat and the Red Sea: An Account of Similarities and Differences. In *Aqaba–Eilat, the Improbable Gulf: Environment, Biodiversity and Preservation*; Por, F.D., Ed.; Hebrew University Magnes Press: Jerusalem, Israel, 2008; pp. 177–188.
22. Gul, S. New records of nudibranchs (Gastropoda: Heterobranchia) from the coast of Pakistan (Northern Arabian Sea). *Festivus* **2019**, *51*, 114–124. [[CrossRef](#)]
23. Sreeraj, C.R.; Sivaperuman, C.; Raghunathan, C. Addition to the opisthobranchiate (Opisthobranchia, Mollusca) fauna of Andaman and Nicobar Islands, India. *Galaxea* **2012**, *14*, 105–113. [[CrossRef](#)]
24. Sreeraj, C.R.; Sivaperuman, C.; Raghunathan, C. An annotated checklist of opisthobranch fauna (Gastropoda: Opisthobranchia) of the Nicobar Islands, India. *J. Threat. Tax* **2012**, *4*, 2499–2509. [[CrossRef](#)]
25. Sreeraj, C.R.; Sivaperuman, C.; Raghunathan, C. Species Diversity and Abundance of Opisthobranch Molluscs (Gastropoda: Opisthobranchia) in the Coral Reef Environments of Andaman and Nicobar Islands, India. In *Ecology and Conservation of Tropical Marine Faunal Communities*; Venkataraman, K., Sivaperuman, C., Raghunathan, C., Eds.; Springer: Berlin/Heidelberg, Germany, 2013; pp. 81–106.
26. Tibiriçá, Y.; Pola, M.; Cervera, J.L. Astonishing diversity revealed: An annotated and illustrated inventory of Nudipleura (Gastropoda: Heterobranchia) from Mozambique. *Zootaxa* **2017**, *4359*, 1–133. [[CrossRef](#)]
27. Gosliner, T.M.; Kuzirian, A. Two new species of Flabellinidae (Opisthobranchia: Aeolidacea) from Baja California. *Proc. Cal. Acad. Sci.* **1990**, *47*, 1–15.
28. Gosliner, T.M.; Willan, R.C. Review of the Flabellinidae (Nudibranchia: Aeolidacea) from the tropical Indo–Pacific, with descriptions of five new species. *Veliger* **1991**, *34*, 97–133.
29. Martynov, A.V.; Korshunova, T.A. Opisthobranch molluscs of Vietnam (Gastropoda: Opisthobranchia). In *Benthic Fauna of the Bay of Nhatrang, Southern Vietnam*; Britayev, T.A., Pavlov, D.S., Eds.; KMK Scientific Press: Moscow, Russia, 2012; Volume 2, pp. 142–257.
30. Yonow, N. Results of the Rumphius Biohistorical Expedition to Ambon (1990). Part 16. The Nudibranchia—Dendronotina, Arminina, Aeolidina, and Doridina (Mollusca: Gastropoda: Heterobranchia). *Arch. Für Molluskenkd.* **2017**, *146*, 135–172. [[CrossRef](#)]
31. Papu, A.; Undap, N.; Martinez, N.A.; Segre, M.R.; Kuada, R.R.; Perin, M.; Yonow, N.; Wägele, H. First Study on Marine Heterobranchia (Gastropoda, Mollusca) in Bangka Archipelago, North Sulawesi, Indonesia. *Diversity* **2020**, *12*, 52. [[CrossRef](#)]
32. Jung, D.; Park, J.K. First report of an aeolid nudibranch *Flabellina athadona* and an identification key for the genus *Flabellina* from Korea. *Korean J. Malacol.* **2015**, *31*, 249–252. [[CrossRef](#)]
33. Baba, K. *Opisthobranchia of Sagami Bay*; Iwanami Shoten: Tokyo, Japan, 1955; p. 59.

34. Wells, F.E.; Bryce, C.W. *Sea Slugs of Western Australia*; Western Australian Museum: Perth, Australia, 1993; p. 184.
35. Burn, R. A checklist and bibliography of the Opisthobranchia (Mollusca: Gastropoda) of Victoria and the Bass Strait area, south-eastern Australia. *Mus. Vict. Sci. Rep.* **2006**, *10*, 7–13. [[CrossRef](#)]
36. Larkin, M.F.; Smith, S.D.; Willan, R.C.; Davis, T.R. Diel and seasonal variation in heterobranch sea slug assemblages within an embayment in temperate eastern Australia. *Mar. Biodivers.* **2018**, *48*, 1541–1550. [[CrossRef](#)]
37. Gosliner, T.M.; Behrens, D.W.; Valdés, Á. *Indo-Pacific Nudibranchs and Sea Slugs: A Field Guide to The World's Most Diverse Fauna*; Sea Challengers Natural History Books; California Academy of Sciences: San Francisco, CA, USA, 2008; p. 426.
38. Korshunova, T.; Martynov, A.; Bakken, T.; Evertsen, J.; Fletcher, K.; Mudianta, I.W.; Saito, H.; Lundin, K.; Schroedl, M.; Picton, B. Polyphyly of the traditional family Flabellinidae affects a major group of Nudibranchia: Aeolidacean taxonomic reassessment with descriptions of several new families, genera, and species (Mollusca, Gastropoda). *ZooKeys* **2017**, *717*, 1. [[CrossRef](#)] [[PubMed](#)]
39. Ekimova, I.A.; Antokhina, T.I.; Schepetov, D.M. Molecular data and updated morphological description of *Flabellina rubrolineata* (Nudibranchia: Flabellinidae) from the Red and Arabian seas. *Ruthenica* **2020**, *30*, 183–194. [[CrossRef](#)]
40. Gosliner, T.M.; Valdés, Á.; Behrens, D.W. *Nudibranch & Sea Slug Identification: Indo-Pacific*, 2nd ed.; New World Publications: Jacksonville, FL, USA, 2018; p. 452.
41. Goodheart, J.A.; Bazinet, A.L.; Valdés, Á.; Collins, A.G.; Cummings, M.P. Prey preference follows phylogeny: Evolutionary dietary patterns within the marine gastropod group Cladobranchia (Gastropoda: Heterobranchia: Nudibranchia). *BMC Evol. Biol.* **2017**, *17*, 1–14. [[CrossRef](#)]
42. Valdés, Á.; Lundsten, L.; Wilson, N.G. Five new deep-sea species of nudibranchs (Gastropoda: Heterobranchia: Cladobranchia) from the Northeast Pacific. *Zootaxa* **2018**, *4526*, 401–433. [[CrossRef](#)]
43. Ekimova, I.A.; Antokhina, T.I.; Schepetov, D.M. “Invasion” in the Russian Arctic: Is global Climate Change a real driver? A remarkable case of two nudibranch species. *Ruthenica* **2019**, *29*, 103–113.
44. Ekimova, I.; Valdés, Á.; Malaquias, M.A.E.; Rauch, C.; Chichvarkhin, A.; Mikhlina, A.; Antokhina, T.; Chichvarkhina, O.; Schepetov, D. High-level taxonomic splitting in allopatric taxa causes confusion downstream: A revision of the nudibranch family Coryphellidae. *Zool. J. Linn. Soc. Lond.* **2022**, 1–35. [[CrossRef](#)]
45. Furfaro, G.; Salvi, D.; Trainito, E.; Vitale, F.; Mariottini, P. When morphology does not match phylogeny: The puzzling case of two sibling nudibranchs (Gastropoda). *Zool. Scr.* **2021**, *50*, 439–454. [[CrossRef](#)]
46. Ekimova, I.A. A new species of the genus *Coryphella* (Gastropoda: Nudibranchia) from the Kuril Islands. *Ruthenica* **2022**, *32*, 41–48. [[CrossRef](#)]
47. Ivanova, N.V.; Dewaard, J.R.; Hebert, P.D.N. An inexpensive, automation-friendly proto-col for recovering high-quality DNA. *Mol. Ecol. Notes* **2006**, *6*, 998–1002. [[CrossRef](#)]
48. Osterburg, H.H.; Allen, J.K.; Finch, C.E. The use of ammonium acetate in the precipitation of ribonucleic acid. *Biochem. J.* **1975**, *147*, 367–368. [[CrossRef](#)] [[PubMed](#)]
49. Folmer, O.; Black, M.; Hoeh, W.; Lutz, R.; Vrijenhoek, R. DNA primers for amplification of mitochondrial cytochrome c oxidase subunit I from diverse metazoan invertebrates. *Mol. Mar. Biol. Biotechnol.* **1994**, *3*, 294–299. [[PubMed](#)]
50. Palumbi, S.; Martin, A.; Romano, S.; McMillan, W.O.; Stice, L.; Grabowski, G. *The Simple Fool's Guide to PCR*; Version 2.0; University of Hawaii: Honolulu, HI, USA, 1991.
51. Puslednik, L.; Serb, J.M. Molecular phylogenetics of the Pectinidae (Mollusca: Bivalvia) and effect of increased taxon sampling and outgroup selection on tree topology. *Mol. Phylogenet. Evol.* **2008**, *48*, 1178–1188. [[CrossRef](#)]
52. Colgan, D.J.; McLauchlan, A.; Wilson, G.D.F.; Livingston, S.P.; Edgecombe, G.D.; Macaranas, J.; Gray, M.R. Histone H3 and U2 snRNA DNA sequences and arthropod molecular evolution. *Aust. J. Zool.* **1998**, *46*, 419–437. [[CrossRef](#)]
53. Lê, H.L.; Lecointre, G.; Perasso, R. A 28S rRNA-based phylogeny of the gnathostomes: First steps in the analysis of conflict and congruence with morphologically based cladograms. *Mol. Phylogenet. Evol.* **1993**, *2*, 31–51. [[CrossRef](#)] [[PubMed](#)]
54. Kearse, M.; Moir, R.; Wilson, A.; Stones-Havas, S.; Cheung, M.; Sturrock, S.; Drummond, A. Geneious Basic: An integrated and extendable desktop software platform for the organization and analysis of sequence data. *Bioinformatics* **2012**, *28*, 1647–1649. [[CrossRef](#)] [[PubMed](#)]
55. Altschul, S.F.; Gish, W.; Miller, W.; Myers, E.W.; Lipman, D.J. Basic local alignment search tool. *J. Mol. Biol.* **1990**, *215*, 403–410. [[CrossRef](#)]
56. Edgar, R.C. MUSCLE: Multiple sequence alignment with high accuracy and high throughput. *Nucleic Acids Res.* **2004**, *32*, 1792–1797. [[CrossRef](#)] [[PubMed](#)]
57. Kumar, S.; Stecher, G.; Tamura, K. MEGA7: Molecular evolutionary genetics analysis version 7.0 for bigger datasets. *Mol. Biol. Evol.* **2016**, *33*, 1870–1874. [[CrossRef](#)]
58. Chaban, E.M.; Ekimova, I.A.; Schepetov, D.M.; Chernyshev, A.V. *Meloscaplander grandis* (Heterobranchia: Cephalaspidea), a deep-water species from the North Pacific: Redescription and taxonomic remarks. *Zootaxa* **2019**, *4646*, 385–400. [[CrossRef](#)]
59. Darriba, D.; Posada, D.; Kozlov, A.M.; Stamatakis, A.; Morel, B.; Flouri, T. ModelTest-NG: A new and scalable tool for the selection of DNA and protein evolutionary models. *Mol. Biol. Evol.* **2020**, *37*, 291–294. [[CrossRef](#)] [[PubMed](#)]
60. Flouri, T.; Izquierdo-Carrasco, F.; Darriba, D.; Aberer, A.J.; Nguyen, L.T.; Minh, B.Q.; von Haeseler, A.; Stamatakis, A. The Phylogenetic Likelihood Library. *Syst. Biol.* **2014**, *64*, 356–362. [[CrossRef](#)] [[PubMed](#)]
61. Ronquist, F.; Huelsenbeck, J.P. MrBayes 3: Bayesian phylogenetic inference under mixed models. *Bioinformatics* **2003**, *19*, 1572–1574. [[CrossRef](#)] [[PubMed](#)]

62. Stamatakis, A. RAxML version 8: A tool for phylogenetic analysis and post-analysis of large phylogenies. *Bioinformatics* **2014**, *30*, 1312–1313. [[CrossRef](#)] [[PubMed](#)]
63. Puillandre, N.; Brouillet, S.; Achaz, G. ASAP: Assemble species by automatic partitioning. *Mol. Ecol. Resour.* **2021**, *21*, 609–620. [[CrossRef](#)]
64. Herbert, P.D.N.; Cywinska, A.; Ball, S.L.; DeWaard, J.R. Biological identifications through DNA barcodes. *Proc. R. Soc. Ser. B Bio.* **2003**, *270*, 313–321. [[CrossRef](#)]
65. Zhang, J.; Kapli, P.; Pavlidis, P.; Stamatakis, A. A general species delimitation method with applications to phylogenetic placements. *Bioinformatics* **2013**, *29*, 2869–2876. [[CrossRef](#)]
66. Pons, J.; Barraclough, T.G.; Gomez-Zurita, J.; Cardoso, A.; Duran, D.P.; Hazell, S.; Kamoun, S.; Sumlin, W.D.; Vogler, A.P. Sequence-based species delimitation for the DNA taxonomy of undescribed insects. *Syst. Biol.* **2006**, *55*, 595–609. [[CrossRef](#)]
67. Fujisawa, T.; Barraclough, T.G. Delimiting species using single-locus data and the Generalized Mixed Yule Coalescent approach: A revised method and evaluation on simulated data sets. *Syst. Biol.* **2013**, *62*, 707–724. [[CrossRef](#)]
68. Bouckaert, R.; Vaughan, T.G.; Barido-Sottani, J.; Duchêne, S.; Fourment, M.; Gavryushkina, A.; Heled, J.; Jones, G.; Kühnert, D.; De Maio, N.; et al. BEAST 2.5: An advanced software platform for Bayesian evolutionary analysis. *PLoS Comput. Biol.* **2019**, *15*, e1006650.
69. Furfaro, G.; Salvi, D.; Mancini, E.; Mariottini, P. A multilocus view on Mediterranean aeolid nudibranchs (Mollusca): Systematics and cryptic diversity of Flabellinidae and Piseinotecidae. *Mol. Phylogenet. Evol.* **2018**, *118*, 13–22. [[CrossRef](#)] [[PubMed](#)]
70. Wilson, N.G.; Burghardt, I. Here be dragons-phylogeography of *Pteraeolidia ianthina* (Angas, 1864) reveals multiple species of photosynthetic nudibranchs (Aeolidina: Nudibranchia). *Zool. J. Linn. Soc. Lond.* **2015**, *175*, 119–133. [[CrossRef](#)]
71. Korshunova, T.; Mehrotra, R.; Arnold, S.; Lundin, K.; Picton, B.; Martynov, A. The formerly enigmatic Unidentiidae in the limelight again: A new species of the genus *Unidentia* from Thailand (Gastropoda: Nudibranchia). *Zootaxa* **2019**, *4551*, 556–570. [[CrossRef](#)] [[PubMed](#)]
72. Matsuda, S.B.; Gosliner, T.M. Glossing over cryptic species: Descriptions of four new species of *Glossodoris* and three new species of *Doriprismatica* (Nudibranchia: Chromodorididae). *Zootaxa* **2018**, *4444*, 501–529. [[CrossRef](#)] [[PubMed](#)]
73. Soong, G.Y.; Bonomo, L.J.; Reimer, J.D.; Gosliner, T.M. Battle of the bands: Systematics and phylogeny of the white *Goniobranthus* nudibranchs with marginal bands (Nudibranchia, Chromodorididae). *ZooKeys* **2022**, *1083*, 169. [[CrossRef](#)] [[PubMed](#)]
74. Marshall, J.G.; Willan, R.C. *Nudibranchs of Heron Island, Great Barrier Reef*; Backhuys Publishers: Leiden, The Netherlands, 1999; p. 257.
75. Herve, J.-F. *Guide des Nudibranches de Nouvelle-Caledonie et autres Opisthobranches*; Editions Catherine Ledru: Noumea, France, 2010; p. 403.
76. Cheney, K.L.; Cortesi, F.; How, M.J.; Wilson, N.G.; Blomberg, S.P.; Winters, A.E.; Marshall, N.J. Conspicuous visual signals do not coevolve with increased body size in marine sea slugs. *J. Evolut. Biol.* **2014**, *27*, 676–687. [[CrossRef](#)] [[PubMed](#)]